BULLETIN OF THE ASTRONOMICAL INSTITUTES OF THE NETHERLANDS

1954 MAY 14 VOLUME XII NUMBER 452

COMMUNICATION FROM THE NETHERLANDS FOUNDATION FOR RADIO ASTRONOMY AND THE OBSERVATORY AT LEIDEN

THE SPIRAL STRUCTURE OF THE OUTER PART OF THE GALACTIC SYSTEM DERIVED FROM THE HYDROGEN EMISSION AT 21 cm WAVE LENGTH

BY H. C. VAN DE HULST, C. A. MULLER AND J. H. OORT

A discussion is given of the equipment used to measure the line emission at 21 cm of interstellar hydrogen, and of the observations made up to the summer of 1953. The measures were made with a 7.5-metre paraboloid, movable around a vertical and a horizontal axis. It can be pointed to a given position with an accuracy of about 0°.1. The beam width between half-power points is 1°.9 in horizontal and 2°.7 in vertical direction. The receiver is based on the principle of switching at a rate of 430 c/s between two frequencies 648 kc/s apart. The band width for both frequencies was 40 kc/s, or 8.4 km/sec. The noise figure of the receiver as used for the series of measures discussed in the present article was 10. (sections 2 and 3).

Measures of line profiles were made in the galactic plane at points spaced 5° in longitude. They are shown in Figures 5 and 6, and in Table 1. They have been reduced as well as possible to the same intensity scale, the unit of intensity corresponding to about 1°.0 K. The estimated uncertainty in the strongest intensities is of the order of 5%, and 1 or 2 km/sec in the velocities. (sections 4–9).

The velocities have all been corrected for the orbital motion of the earth and for the motion of the sun, for which the standard values $v = 20$ km/sec, towards 18^h0^m, $+30°.0$ were adopted. These were shown to be in agreement with the data given by early-type stars and interstellar absorption lines, and are, to some extent, corroborated by the 21-cm results (section 10). For the position of the galactic pole we have used 12^h40^m, $+28°.0$, the pole used by OHLSSON in the Lund tables. The 21-cm data indicate that a correction of about 1°.5 is needed to this pole. The direction of the galactic centre has been assumed at 327° longitude. Recent 21-cm results indicate that the true position must be near $l = 328°.0$, $b = -1°.5$. (section 11). From the present measures a distance to the centre of 8.26 kps has been derived, in close agreement with recent estimates by BAADE. The following values were adopted for the region around the sun: distance to centre $R_0 = 8.2$ kps, velocity of rotation $\Theta_0 = 216$ km/sec, angular rotation $\omega_0 = A - B = 26.4$ km/sec.kps, $d\omega/dR = -2A/R_0 = -4.76$ km/sec.kps^2. A and B are the ordinary constants of differential rotation, for which we assumed $A = +19.5$, $B = -6.9$ km/sec.kps. (section 12).

From the low-frequency edges of the profiles observed between 345° and 40° longitude the angular velocity of rotation of the Galactic System at different distances from the centre was deduced. Provisional values of $\omega(R)$ and $\Theta_c(R)$ are given in Figures 8 and 9. From these the relation between mean radial velocity, V_g, and distance from the sun, r, has been derived. Samples of these relations are in Figure 10. (sections 12—14). For the region outside the circle with radius R_0 the points of maximum and minimum intensity in the line profiles could thus be located in space as points of maximum and minimum hydrogen density (Figure 11). The principal uncertainty in this graph is caused by the assumption that the gravitational field of force in the galactic plane is radially symmetrical. The points of maximum density are seen to be arranged in spiral arms, which seem to be only little inclined. Wherever they are inclined the direction is such that they wind up during the rotation. (section 15).

The average temperature of the neutral interstellar hydrogen was found to be 110° K. (More recent measurements indicate a somewhat higher value, of around 125°). The observations show that, in the absence of galactic rotation the absorption coefficient in the centre of the line averages 0.95 kps^{-1}, for the band width used. For zero band width it would be 1.20 kps^{-1}. In almost all directions the galactic rotation prevents the gas from becoming optically thick. Except for one observation in the dark clouds in Taurus (see section 9) no evidence was found for considerable systematic differences in temperature. This statement applies only to the outer regions discussed in the present article. In the innermost part a drop of temperature, or a decreasing density of hydrogen atoms, are indicated by the relatively low 21-cm intensities observed for these regions. (section 16).

We have attempted to derive the true density distribution in the galactic plane by correcting statistically for the random motions of the clouds. The random radial motions were assumed to be distributed as suggested by BLAAUW (formula (17)). The average random radial velocity was found to be 8.5 km/sec. (section 17). The resulting density distribution is shown in Figures 15 and 16. For the principal arms between 65° and 220° longitude the maximum density averages about 1.4 H/cm^3, except for the part of the 'Perseus' arm that is situated between 97° and 123°, where it is 2.7. Between the arms the density appears mostly negligible. The distance between the points in the Perseus arm where the density has dropped to half the maximum value, measured in the galactic plane in a direction perpendicular to the arm, is roughly 0.8 kps. The space between the arms, measured between the half-density points, varies from about 1.3 to 2 kps. From observations between 50° and 220° longitude the total average density in the ring between $R = 8.2$ and $R = 11.2$ is found to be 0.70 H/cm^3. It is not unlikely that the ordinary photographic absorption coefficient is roughly proportional to n_H, and that its variation can thus be inferred from Figure 16. (section 18). In the last section a comparison has been made with other results on large-scale distribution of interstellar gas and early-type giants.

1. *Introduction.*

The possibility that an emission line of hydrogen at 21 cm wave length would be emitted in observable strength by interstellar clouds was first suggested by VAN DE HULST during a symposium on radio astronomy held in Leiden in 1944[1]). The line arises from the transition between the hyperfine structure levels of the ground state of atomic hydrogen. At that time informal plans had already been made to start radio-astronomical work in the Netherlands with a larger antenna than had been used by REBER in his pioneer investigations of the continuous galactic radiation. Right after the war a project was submitted for a movable 25-metre paraboloid, but the realization had to be delayed, mainly because of the serious shortage of radio engineers in the Netherlands at that epoch. A first attempt to observe the 21-cm line was started in 1948 by Mr H. Hoo, with a war-surplus receiver kindly put at our disposal for this purpose by Prof. C. J. GORTER at Leiden. Because of lack of suitable instruments and lack of experience, progress was slow. Moreover, in March 1950 the entire receiver was destroyed by fire. A new receiver was developed and built at the laboratory of the Philips Factory in Eindhoven, under the direction of Dr F. L. STUMPERS. It was completed and considerably changed by MULLER, who had succeeded Mr Hoo toward the end of 1950. In the spring of 1951 MULLER made his first measures of the 21-cm line, 1½ months after the first experimental evidence of the presence of this interstellar emission line was obtained by EWEN and PURCELL[2]).

The writers recall with pleasure the valuable information and friendly co-operation received from Drs EWEN and PURCELL, and from Dr F. KERR, who was our liaison with the Australian group. A similar co-operation has continued among all workers in this field; one of its results is the exchange of a regular "1420 Mc/s newsletter", edited at Leiden.

A detailed investigation of the intensity distribution in this line seemed extremely promising for galactic research. For this line combines the advantages of galactic radio astronomy in general, which is the penetration of the dust clouds out into the farthest regions of our Galaxy, with the advantage of a well-defined spectral line, which is the possibility to measure radial velocities. These considerations have dictated the choice of our first programme.

The work described in the following article was carried out under the auspices of the Netherlands Foundation for Radio Astronomy. The board of directors of this foundation consists of representatives of the observatories of Leiden, Utrecht and Groningen, of the Netherlands Post and Telegraph Service (P.T.T.), of the Physical Laboratory of the Philips Factories at Eindhoven and of the Royal Meteorological Institute at De Bilt. All the financial support was provided by the Netherlands Organization for Pure Research (Z.W.O.).

We are greatly indebted to the extremely helpful co-operation of all members of the board of directors of the Foundation for Radio Astronomy, without whose unfailing interest and assistance the present progress could not have been achieved. Particular gratitude is due to Mr DE VOOGT, through whose foresight two Würzburg paraboloids were rescued from destruction on the sea coast. It was by his courtesy and that of the director general of the P.T.T. that one of these, re-erected at the P.T.T. transmitting station in Kootwijk, was made available for the 21-cm work.

This paper describes the results of a year of observations, from July 1952, when an improved receiver was put into operation, to June 1953, interrupted by periods of instrumental checks and improvements.

After important improvements in the receiver, observations were started again in November 1953 and have been continued since, with only minor interruptions. New line profiles are being obtained at $b = 0°$ for every $2\frac{1}{2}°$ in longitude, while at each 5° profiles are observed at various latitudes between $-10°$ and $+10°$. Beside these programmes observations have been concentrated especially on the more central regions of the Galaxy.

Brief accounts of the results reported in this paper have been given in an early stage [3]) [4]) [5]) and in a more advanced stage [6]) [7]) [8]) [9]). Other papers on the 21-cm line include an early theoretical paper by SHKLOVSKY [10]) and an observational [11]) and a theoretical [12]) study from Australia.

The three authors, whose names appear in alphabetical order, have taken about equal shares in the work, MULLER being chiefly responsible for the instrument and the observations, VAN DE HULST for the reduction and OORT for the astronomical discussion. At various phases the authors have been assisted by

---

[1]) H. C. VAN DE HULST, *Ned. Tijdschr. v. Natuurkunde* **11**, 201, 1945.

[2]) For an account of the early observations see H. I. EWEN and E. M. PURCELL; C. A. MULLER and J. H. OORT; J. L. PAWSEY; all in *Nature* **168**, 356–358, 1951.

[3]) C.A. MULLER, *Tijdschrift v. h. Ned. Radiogenootschap* **17**, 3, 1952.

[4]) J. H. OORT, *Transactions I. A. U.* **8** (meeting Rome 1952).

[5]) J. H. OORT, *Versl. Kon. Ned. Ak. Wet. Amsterdam* **61**, 140, 1952.

[6]) H. C. VAN DE HULST, *Akademiedagen* **6**, 115, 1953.

[7]) H. C. VAN DE HULST, *Observatory* **73**, 129, 1953.

[8]) J. H. OORT, *Ciel et Terre* **59**, 117, 1953.

[9]) J. H. OORT, *Die Naturwissenschaften* **41**, 73, 1954.

[10]) I. S. SHKLOVSKY, *Astronomicheskii Zhurnal* **26**, 10, 1949.

[11]) W. N. CHRISTIANSEN and J. V. HINDMAN, *Australian J. Sci. Res.* A. **5**, 437, 1952 and *Observatory* **72**, 149, 1952.

[12]) P. WILD, *Ap. J.* **115**, 206, 1952.

several of the astronomy students at Leiden, in particular by Messrs WOLTERBEEK MULLER, VAN WOERDEN, KWEE, WESTERHOUT and SCHMIDT.

Part I. INSTRUMENTS AND OBSERVATIONS.

2. *The antenna.*

The antenna is an old German radar mirror of the well-known "giant Würzburg" type: a paraboloid of 7.5 metre aperture and 1.7 metre focal length. It is mounted in an altazimuth mounting at the P.T.T. transmission station at Kootwijk. The original cabin contains the receiver and recorder, and serves as a counter weight of the paraboloid. Together they are mounted on a concrete base at the centre of which is the vertical axis of rotation.

The feed consists of a half-wave dipole and reflector disk in the focus of the paraboloid. A rigid air-insulated co-axial line connects the feed with the front end of the receiver, mounted behind the reflecting surface of the antenna.

For a wave length of 21.1 cm the beam width, between half-power points, is 1°.9 in horizontal direction and 2°.7 in vertical direction. Figure 1 shows the antenna diagrams in the two directions.

FIGURE 1

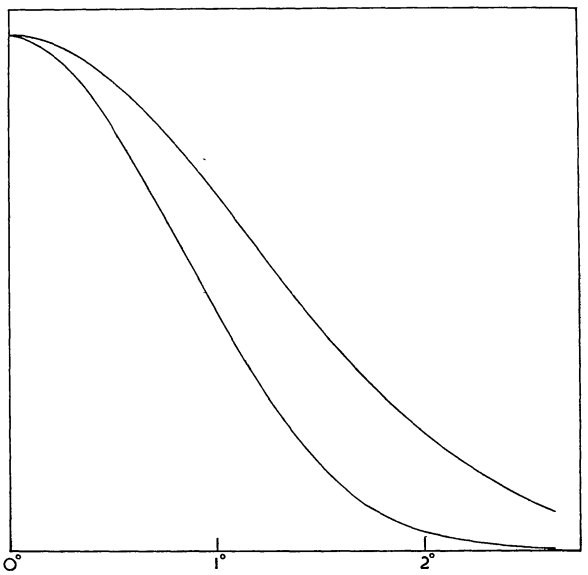

Main lobe of antenna diagram in horizontal (lower curve) and vertical direction (upper curve).

The antenna had been erected before it was clear that an accuracy of the order of 0°.1 would be desirable in most measurements. Therefore a number of checks were made to make sure that the antenna could be pointed at a known region of the sky with that accuracy. These checks were:

a. New circles with divisions of 0°.5 were mounted and checked. Readings can be made by interpolation to 0°.1.

b. A determination of the radio axis of the telescope was made. The symmetry axis of the antenna pattern is defined as the radio axis of the telescope. Fixed to the paraboloid is a sight and a small telescope, which define the optical axis. When the pipe carrying the dipole had been placed as well as possible along the geometrical axis of the paraboloid and the telescope parallel to it, the radio axis was determined by observations of the sun. A number of measurements gave deviations from the optical axis well below 0°.1.

c. The direction of the vertical axis was determined by means of a level put on the floor of the cabin, while the cabin was rotated to various positions.

Result: $A = 103° \pm 2°$ and $h = 89°.72 \pm 0°.01$.

The geographical co-ordinates are $\varphi = 52°10'.2$ and $\lambda = -5°50'.7$. The deviating direction of the vertical axis corresponds to the real vertical at a slightly different geographical location: $\varphi' = 52°14'.0$ and $\lambda' = -5°24'.0$.

d. The direction of the horizontal axis of rotation was determined by turning the telescope around the vertical axis and by measuring in various positions the vertical distances from markers on the horizontal axis to fixed markers on the ground. The result is that the slope with respect to a plane perpendicular to the vertical axis is 0°.04, the right end being higher. This difference was neglected.

e. The corrections to be applied to h and A read from the circle, in order to obtain the real h and A were computed from the measured deviations of the vertical axis.

f. The positions of dozens of bright stars were determined during several nights by pointing with the telescope and reading the circles. These measurements revealed no further systematic differences except a small scale-error in the division of the h-circle.

g. A final table of corrections was made and used in making the settings of the radiotelescope.

3. *The receiver.*

The present receiver, like the earlier one used in 1951 [1]), is based on the switching principle, first introduced by DICKE [2]). The receiver is being switched between two frequencies 648 kc/s apart, at a rate of 430 c/s, and the intensity difference between the two frequencies is measured. The two frequencies can be moved together through a 3 Mc/s wide band around the frequency of the hydrogen line.

[1]) C. A. MULLER and J. H. OORT, *Nature* **168**, 357, 1951.
[2]) R. H. DICKE, *Rev. Sci Instr.* **17**, 268, 1946.

FIGURE 2

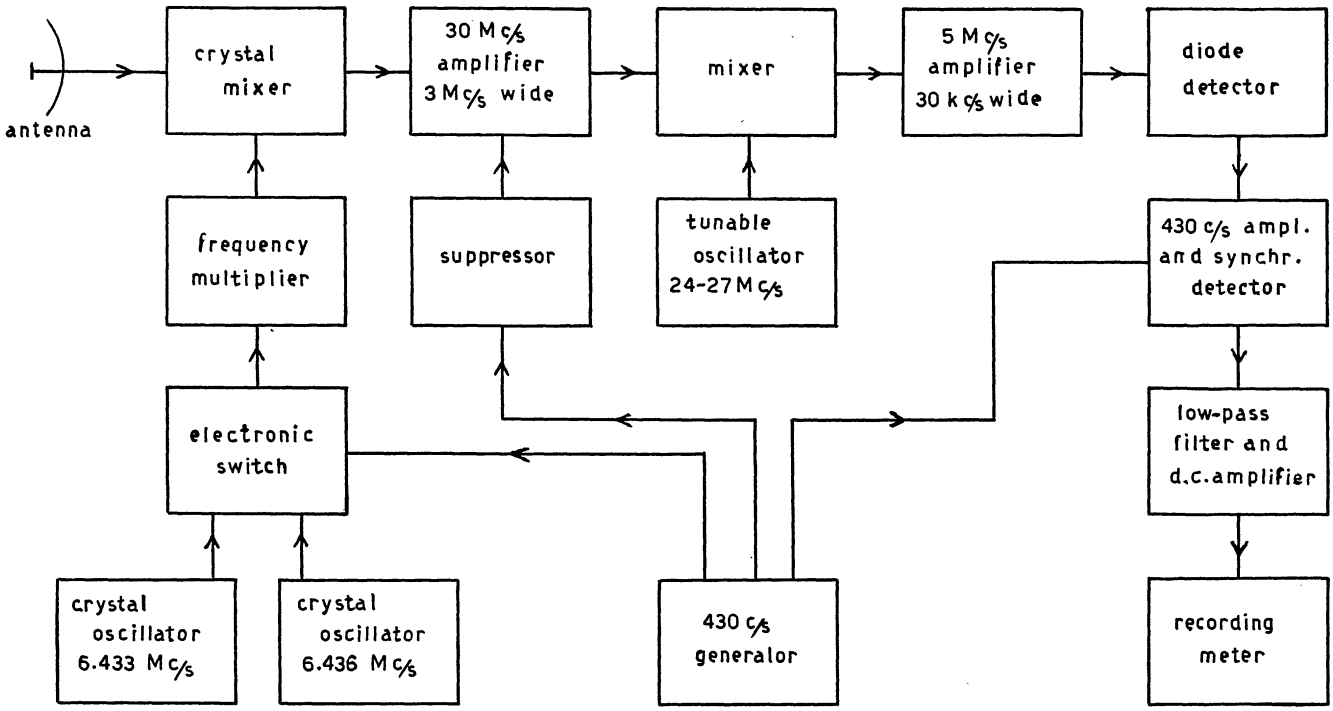

Block diagram of receiver

The receiver (see Figure 2) is of the superheterodyne type, with double frequency conversion. The switching takes place between two crystal-controlled frequencies in the first local oscillator by means of an electronic switch driven by a 430 c/s oscillator. The difference between the two frequencies can be changed from 100-700 kc/s. During the set of observations reported in this paper the setting was not changed, but the actual frequency interval showed slow variations (see section 6).

The first intermediate-frequency amplifier has a 3 Mc/s pass band around 30 Mc/s. The second intermediate-frequency amplifier is tuned to 5 Mc/s and is 40 kc/s wide[1]). This channel determines the band width of the receiver.

The second local oscillator is tunable from 24 to 27 Mc/s. The tuning can be done automatically with a motor at a rate of about 1 Mc/s in one hour, or by hand. The position of the dial attached to the shaft of the tuning condensor was used for reading the frequency of the oscillator.

If the energies received on the two frequencies differ, a 430 c/s component occurs in the rectified output of the receiver. The amplitude of this component is directly proportional to the energy difference, because the difference is small compared to the output energy of the receiver. The 430 c/s component is amplified and then converted to direct current in a synchronous detector. Then follows a low-pass filter, which limits the pass band of the indicator to frequencies below 0.01 c/s (half-power point), and thus determines the time constant of the indicator. To give a value of the time constant would be ambiguous, because different definitions have been used in the literature. The present system corresponds approximately with one giving an exponential approach with a time factor $e^{-t/24\ \mathrm{sec}}$.

The final parts are a d.c. amplifier with the recording meter.

The first mixer uses a Philips M10C germanium crystal, selected for a low noise figure. The noise figure of the receiver has not yet been measured with high accuracy. Preliminary measurements of the energy received from the sun, of the radiation of the earth, and signal-generator measurements, all indicated a noise figure of about $N = 10$ for reception in the signal-frequency channel only.

An independent check of this value by means of an improved antenna system and mixer has been obtained as follows. When this antenna was first pointed at the sky (adopted temperature 0°) and then to the earth (in this case the wooded hill north of the antenna, adopted temperature 300°) a 40% increase of the output energy of the receiver was found. This leads to an upper limit of the noise figure of 3.5 (5.5 db) for reception in both channels (no image rejection is used in the high-frequency part of the receiver) and $N = 7$ (8.5 db) for reception in one channel for the improved

[1]) The block diagram gives erroneously 30 kc/s.

receiver. The line intensities measured with this new receiver and calibrated by means of $N=7$ agree with the line intensities measured with the earlier receiver and calibrated by means of $N=10$. Both lead to the estimate that one unit in the adopted intensity scale corresponds to 1°.0 in brightness temperature (cf. section 7).

Since the noise figure is always determined as an average noise figure for reception in both channels, there may be a small error in the noise figure for reception in one channel due to a possible difference in noise figure between the two channels.

The theoretical limit of detection depends on the fluctuations in the registration, due to the output noise of the receiver. DICKE [1]) has shown, that the r.m.s. fluctuation in the output expressed as a fraction of average receiver power output is given by

$$\Delta T = (N' - 1)\, T_0 \frac{\pi}{2} \sqrt{\frac{\Delta f_m}{\Delta f}}, \qquad (1)$$

where N' is the noise figure for reception in both signal- and image-frequency channels, $T_0 = 290°$ K, Δf_m is the band width of the indicator, and Δf the band width of the receiver. In our case we are receiving in only one channel, so we have to multiply ΔT by two. Using our definition of noise figure we obtain

$$\Delta T = (N - 2 + 2\alpha + \beta)\, T_0 \frac{\pi}{2} \sqrt{\frac{\Delta f_m}{\Delta f}}. \qquad (2)$$

Here αT_0 is the temperature of the background radiation, which is the same in both channels (about 20° at most), and βT_0 is the temperature of the received line radiation (100° at most). We find that α and β are almost negligible, and obtain

$$\Delta T = 2°.2\,\text{K}.$$

The band width of the receiver of 40 kc/s is a compromise between the small band width wanted for accurate line profile measurements, and the required sensitivity. The band width of the indicator should be small for highest sensitivity (the time constant should be high), but it is limited by the tuning rate of the second local oscillator, as can be understood as follows. The smallest observable detail in the line profile is of the order of the band width. When a tuning rate of 1 Mc/s in one hour is used, this band width is passed in about 2 minutes. Since we do not want to lose more detail in the profile than is lost because of the finite band width, the band width of the indicator has to be at least of the order of 1/120 c/s. In our case it was found that the band width of 0.01 c/s gives only a very small distortion of the measured profile. The main influence is that the profile after the low-pass filter lags 24 sec. in respect to the profile before the filter, which is important when measuring the frequency of the line.

[1]) *L.c.*

In general, large changes in the receiver constants, or in sensitivity, do not seem possible, unless a large number of channels is used simultaneously.

Apart from the theoretical limit given by DICKE's formula the accuracy of the measurements can be limited by other factors, because the following requirements have to be met:

a) The receiver shall be identical in both positions of the switch. This means, for instance, that the output of the local oscillator has to be the same on both frequencies, and also, that the output impedance of the antenna system is the same on both frequencies to which the receiver is tuned on the signal- and image-frequency channel. It is rather difficult to fulfil this last demand. The antenna matching in our case was not very good. It caused a shift of the zero of the receiver on the record, which changed somewhat with frequency, but reproduced rather well, especially when temperature and humidity of the antenna system did not change too much.

b) The switching shall have no influence. It was found that switching transients from the local oscillator occur in the i.f. channel, which are not the same for both transitions in one cycle and give a 430-c/s output signal. The influence of these transients has been eliminated by suppressing the i.f. signal during the switching time. The signal is suppressed during about 5 % of the switching cycle.

During the last series of observations frequency calibration of the two crystal frequencies of the first oscillator against a secondary frequency standard was available. This standard is continually compared to the frequency standard of the Netherlands P.T.T. in The Hague. Frequency calibration is possible with an accuracy of about 1 in 10^6.

4. *Methods of observation.*

The problem of obtaining complete observational results on the 21-cm line with a given antenna is one of three-dimensional scanning. We have to measure the intensity as a function of two celestial co-ordinates (e.g. l and b) and the frequency. It is desirable for a clear interpretation to keep either the point in the sky or the frequency fixed during one run. Thus two observing procedures are suggested.

(1) *Line profiles* (see Figure 3). This method was used in most of the cases. The antenna is kept following a point in the sky by changing the position of the antenna every 2.5 minutes. The second local oscillator is tuned automatically with a motor through a frequency band of about 2 Mc/s. By tuning this oscillator the frequencies A and B with their fixed difference are shifted together through the spectrum of the 1420-Mc/s line. If the line profile is narrower than 648 kc/s the true profile is shown two times on the record,

first as a positive deflection, when frequency A is on the line, and next as a negative deflection when frequency B is on the line. If the profile is somewhat wider than the frequency difference, the positive and negative profiles add in the middle of the record, and

FIGURE 3

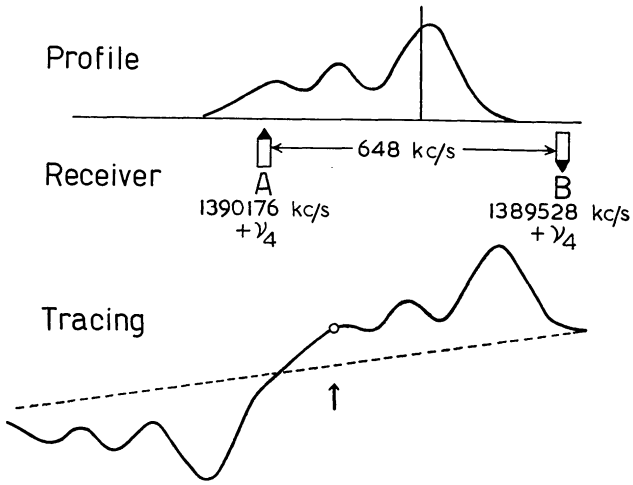

Scheme of measurement of line profile.

the record does not give the true profile. True profiles can be deduced rather easily from the other parts of the record, and the overlapping part gives a check. The noise output of the receiver is kept constant. Positions of the tuning dial are marked on the record by hand. The record gives the measured profile on a linear energy versus a non-linear frequency scale. Some sample tracings are shown in Figure 4.

(2) *Drift curves.* The antenna is held stationary and the frequency of the second local oscillator is held on a fixed value. Time marks are given on the record by hand. The chart gives a record of the energy difference on two fixed frequencies along a line of constant declination. Such measurements can be useful to find the distribution in galactic latitude but in many cases it is desirable to complete them by measures of the line profiles at different latitudes.

5. *Aids to computation.*

In preparing and in reducing the observations a number of simple but time-consuming computations are needed. These computations have to some extent been standardized in the course of this work and some auxiliary tables have been computed. It may be helpful to enumerate here the various aids that are used.

In setting the telescope:

(1) A chronometer of sidereal time, checked against radio time signals using tables of the *Nautical Almanac*.

(2) OHLSSON's tables for conversion of galactic co-ordinates l and b (not changing with precession) into equatorial co-ordinates α and δ (for the year of observation). Compare section 11.

(3) A large-scale rotating map of the sky permitting a conversion into altitude and azimuth, A and h, with an accuracy of 1°.

(4) Master sheets giving A and h for every selected observing point at every half hour of sidereal time at which it is above the horizon.

(5) A little table of corrections to A and h due to imperfect alignment of the telescope. Compare section 2.

(6) Observing sheets, obtained from (4) by linear extrapolation for every five minutes during two hours of observation. The interpolations to $2\frac{1}{2}$ minutes are not written down. Aids (4), (5) and (6) will not be needed with a telescope that follows automatically.

In reducing the observations:

(7) A standard conversion table from scale-reading to frequency. We used a linear table with empirical correction curves. See section 6.

(8) A table of the velocity corrections due to the motions of the earth and the sun. This table required the most laborious computations. Intervals of five days throughout the year were chosen. The velocities were computed for points on the galactic equator at intervals of 5° and points outside the galactic equator that lie on the same declination circle at a difference of $\pm$ one hour in α. See section 10 for details. Some copies of this table are available on request.

6. *The frequency scale.*

To establish the correct frequency scale for the line profiles deduced from each tracing proved to be a long job. Most of the difficulties encountered are not fundamental and have been solved by changes in the equipment since the series of observations discussed in this paper was made. The main trouble was that the values of the crystal-controlled first oscillators could not be accurately maintained, or checked. So empirical corrections had to be derived from line profiles of a same point of the sky observed at different times. Since March 1953 (tracing 346) the values of the two oscillators are maintained at 1389.528 Mc/s (B-oscillator) and 1390.176 Mc/s (A-oscillator). Yet it may useful to describe the earlier procedure in some detail.

The reduction problem is to convert the abscissa x of selected points of a tracing into the frequency ν (in kc/s) with the intermediate step of the dial reading y.

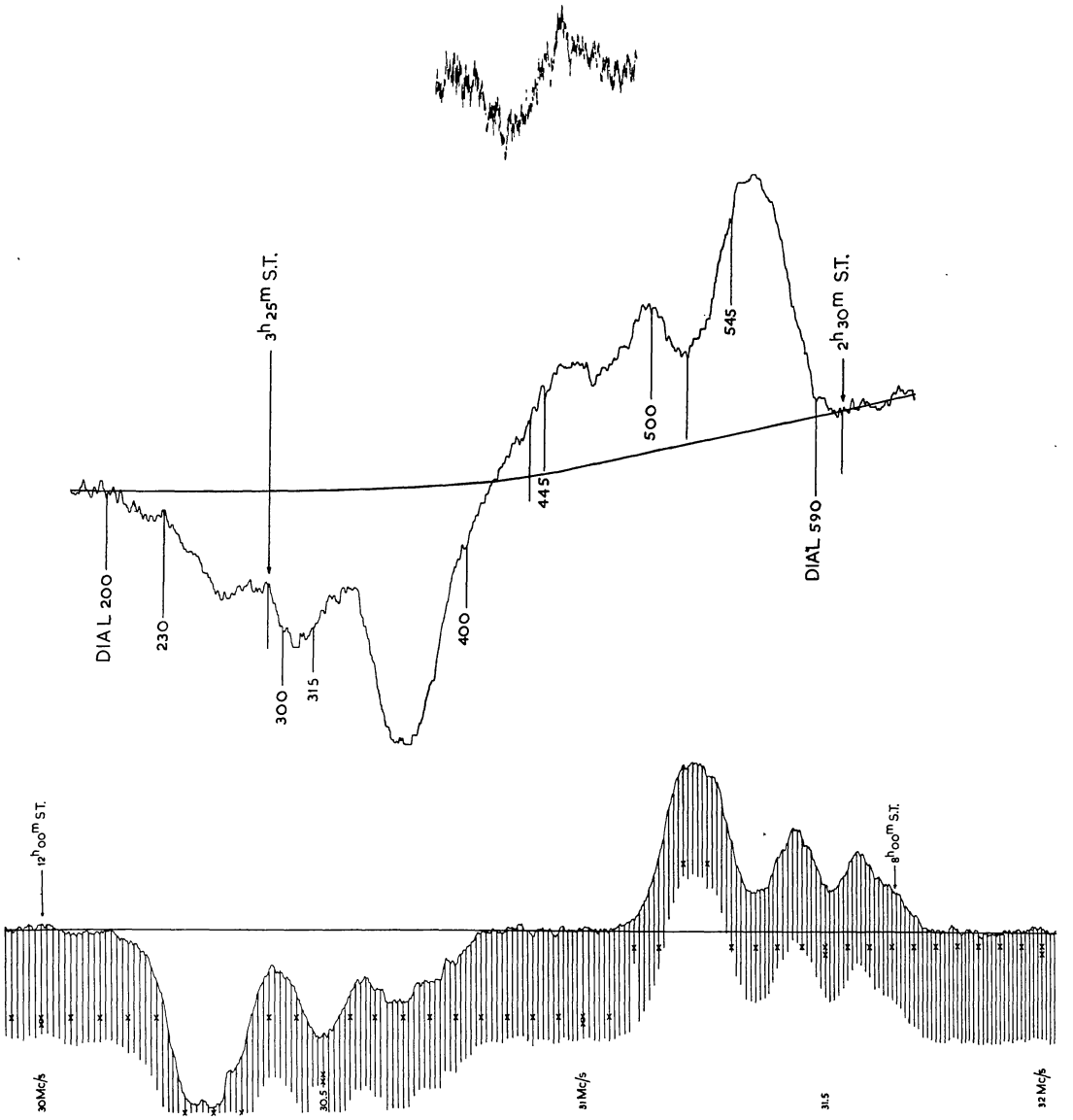

Samples of line profiles. All three refer to a point in the galactic plane at 50° longitude, and are on the same frequency scale. The upper curve was obtained with the first receiver in the summer of 1951. The second shows a sample of the tracings obtained between July 1952 and June 1953, on which the present article is based. Some values of the sideral time and of the dial readings which determine the frequency have been indicated. The frequency increases from right to left. The lower curve shows a profile obtained after November 1953, also with indications of sidereal time and frequency, the latter being now directly given with intervals of 10 kc/s. The frequency increases in a direction opposite to that in the middle curve.

The two conversions were slightly alinear and were linearized by applying small corrections. First, y was not quite linear in x and somewhat erratic; correction curves were made for each individual tracing. Secondly, v is not a linear function of y; the corrections, determined by calibrating the frequency of the second local oscillator, did not change during the entire year. The relation between radial velocity and frequency shift is accurately known and the speed of the paper was one inch in five minutes.

The linear scales are now related as follows:

1 dial unit $=3.400$ kc/s $=0.7182$ km/sec $=$ 0.889 mm $=10.5$ sec, and

1.392 dial units $=4.735$ kc/s $=1$ km/sec $=$ 1.238 mm $=14.6$ sec.

All reductions were made with an accuracy of 0.5 dial units. The band width of the second i.f. channel (corresponding to the slit width of a spectrograph) was 40 kc/s $=8.4$ km/sec. The time lag of 24 seconds reported in section 3 corresponds to 1.6 km/sec.

Frequent changes and improvements in the equipment made it impossible to maintain the first local oscillators at fixed frequencies. Their difference, determined from well-defined peaks or slopes on the tracings, fluctuated between 184 and 195 dial units. The constant value maintained since tracing

FIGURE 4b

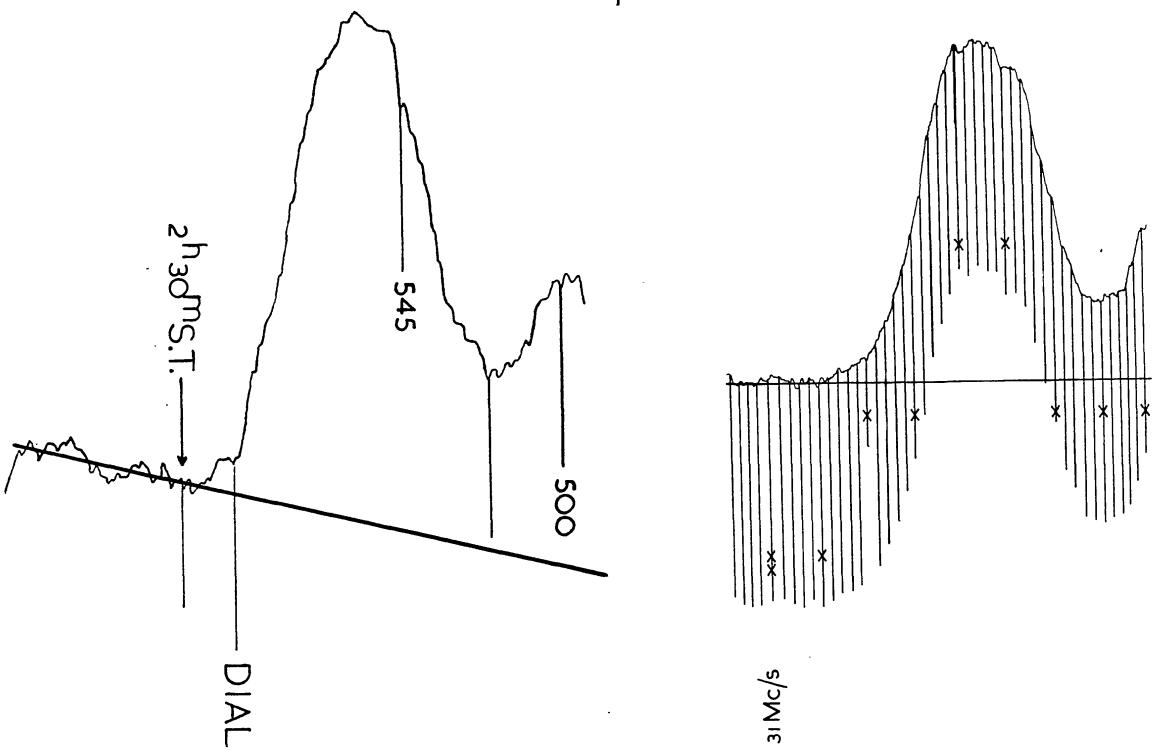

Larger-scale representation of parts of Figure 4a.

number 346 is 648 kc/s = 190.6 units = 137 km/sec.

The basic method for bringing all profiles to a common frequency scale was based on repeated measurements of the same line profile and the determination of empirical corrections for various observing periods. These corrections can be found only after the much larger effect of the earth's orbital velocity has been eliminated. The final uncertainty does not exceed 2 dial units, i.e. 1 or 2 km/sec. The provisional zero for the radial velocity scale was adopted to coincide with the line centre in the directions of $l = 147°$ and $l = 327°$, after the corrections for the velocities of the earth and the sun were applied. The first *absolute* frequency measurements were made in April 1953. They consisted of separate calibrations of the i.f.-amplifier (about 30 Mc/s) and the first local oscillator frequencies (precisely 19.299 and 19.308 Mc/s before multiplication by 72) both against the harmonics of a 100 kc/s crystal. This crystal was tuned with an accuracy of 1 in 10^6 against a 10 kc/s secondary standard that has a better accuracy. The laboratory frequency of the line is known as[1])

$$1420.4056 \pm 0.0003 \text{ Mc/s}.$$

The provisionally adopted line of zero velocity was found by these measurements to agree with a radial velocity of -0.7 km/sec, which does not differ significantly from zero. The frequency calibration has been made fully automatic since then. The zero point of the velocity scale of the results reported in Table 1 and Figures 5 and 6 (section 8) has been chosen in accordance with the new measurements.

1) P. KUSCH and A. G. PRODELL, *Phys. Rev.* **79**, 1009, 1950.

7. *The intensity scale.*

Each profile resulting from the reduction of an individual tracing was plotted in a graph giving the intensity as a function of frequency. The intensity was measured initially as the height h in millimetres above the adopted line of zero intensity. It was multiplied by empirical factors to make the curves of one point in the sky coincide. Then by averaging the A curves and the B curves from each tracing of this point separately (see Figure 3), an average A curve and an average B curve were obtained. The separate treatment of the A and B curves was necessary for those longitudes where the total width of the line exceeds the difference of 650 kc/s, because the left part of the A curve and the right part of the B curve overlap. After corrections for the overlap the A and B curves were averaged giving one curve.

The next step was to multiply the provisional intensities by a factor for each longitude in order to bring them to an intensity scale common to all longitudes. This intensity is denoted by h and is defined by putting the main peak of the standard region ($l = 50°$, $b = 0°$) equal to $h = 100$.

The conversion factors, which rarely fell outside the

FIGURE 5

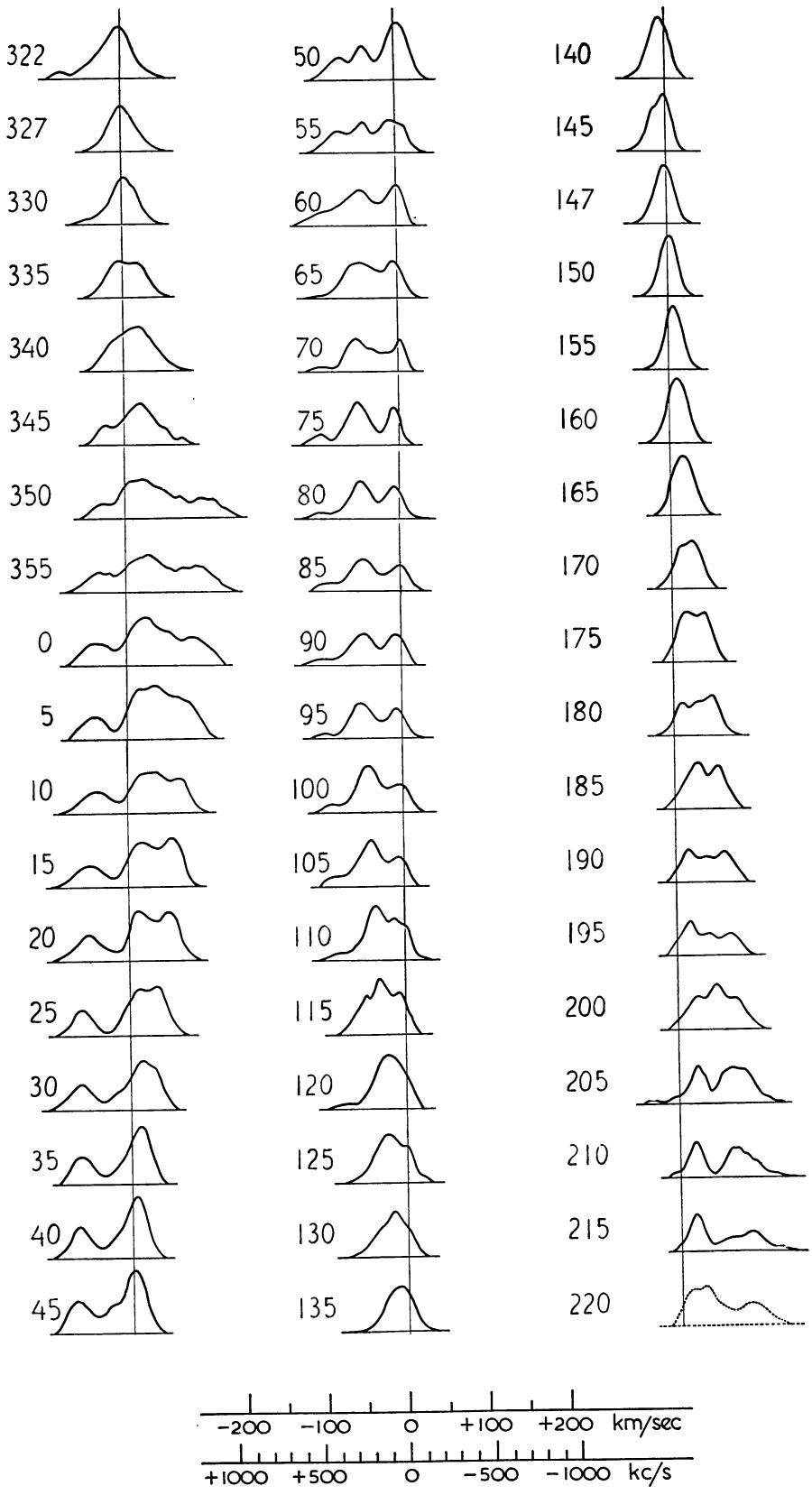

Survey of line profiles at various longitudes.

TABLE I

Line profiles at various galactic longitudes.
The numbers give the measured intensities for the radial velocities V (in km/sec) shown at the top.

l \ V	−120	115	110	105	100	95	90	85	80	75	70	65	60	55	50	45	40	35	30	25	20	15	10	−5	0	+5
220°																						0	9	21	35	52
215																							9	16	26	
210																							7	10	12	22
205																1	5	7	7	6	4	6	10	13	15	20
200																							5	12	20	27
195																						1	7	17	29	40
190																							6	15	25	36
185																						0	6	14	22	31
180																					1	5	10	18	33	50
175																							9	21	34	57
170																					0	6	13	22	35	55
165																					1	7	17	35	62	84
160																			0	4	9	18	35	60	90	107
155																			2	5	9	20	38	65	98	108
150																			3	8	18	38	66	91	104	102
147																	2	5	11	22	40	61	84	100	100	85
145															1	3	6	12	21	37	61	76	83	97	96	74
140															1	4	9	14	26	45	70	92	105	104	90	69
135										0	1	1	2	3	5	11	19	30	47	59	69	75	77	74	63	48
130											3	6	9	14	20	30	39	47	54	63	73	77	68	58	49	37
125										1	4	7	11	17	25	37	50	65	76	82	81	74	66	62	62	46
120						2	3	6	7	9	10	10	11	18	27	38	54	73	85	91	91	86	78	68	55	40
115								0	4	11	19	30	40	51	64	63	72	91	94	82	70	66	71	68	49	34
110					3	5	7	11	13	13	14	18	25	33	52	75	89	92	84	71	65	71	68	63	59	45
105					7	13	17	18	19	19	21	28	39	50	63	74	80	72	57	46	41	45	50	50	43	28
100			0	3	6	11	15	15	14	15	18	25	35	54	72	79	79	72	56	44	42	44	46	48	46	37
95		2	6	10	14	16	16	15	15	21	33	48	58	64	65	62	53	43	35	32	35	45	53	52	42	26
90	2	5	7	9	11	11	11	11	12	15	21	29	38	46	51	53	50	40	31	28	33	44	51	51	47	33
85			0	6	11	12	14	15	15	15	19	27	37	48	53	55	52	44	34	29	29	31	37	43	44	39
80	1	5	5	7	10	11	11	10	11	14	20	30	41	56	64	63	55	44	32	28	35	45	54	55	45	31
75	1	4	10	14	17	19	15	10	10	17	29	42	55	69	74	65	54	42	30	23	24	40	60	64	52	26
70		0	3	5	7	9	9	8	7	9	19	34	47	54	57	51	43	39	38	34	32	32	33	40	53	50
65		1	5	6	7	8	9	12	15	21	29	38	48	57	60	60	59	59	58	54	51	52	59	62	59	48
60	6	10	12	15	19	22	24	26	28	32	36	41	47	52	57	61	59	52	44	39	39	44	53	64	71	64
55			1	3	6	11	16	23	30	35	38	36	33	34	40	47	53	47	36	34	40	50	56	56	54	51
50				0	3	8	14	20	27	34	39	40	34	31	37	50	58	53	42	34	35	48	66	87	97	100
45						3	11	24	40	50	54	53	47	40	33	29	30	34	44	48	51	58	75	95	105	102
40						2	6	12	20	35	47	53	47	39	30	21	17	18	23	30	38	48	60	76	93	103
35							1	10	19	32	42	46	46	42	32	23	16	15	17	22	28	37	49	63	80	93
30					0	3	7	13	20	27	34	42	43	39	32	24	18	14	16	21	27	32	37	45	56	69
25							1	5	10	17	29	40	43	42	34	25	17	9	7	7	12	22	35	47	59	71
20							3	6	10	15	20	27	35	42	44	42	34	28	23	20	17	17	20	33	51	77
15					0	1	2	5	8	13	19	26	31	34	36	36	34	29	24	19	16	18	26	39	52	65
10								0	2	5	8	14	20	26	31	35	37	37	34	29	25	21	21	27	37	48
5											4	12	19	25	31	37	38	38	33	26	17	15	20	32	48	66
0											3	10	17	23	30	35	37	37	36	34	30	26	29	38	47	60
355											2	4	8	13	19	25	30	34	33	31	33	28	30	35	43	50
350														0	5	11	16	22	24	25	24	25	32	45	55	62
345																2	8	17	27	32	32	30	32	37	46	54
340																1	5	11	19	30	41	49	54	60	65	69
335																2	5	10	18	28	40	51	60	62	60	58
330													2	4	6	8	10	13	16	24	30	42	59	72	80	79
322							1	5	10	12	11	9	8	11	16	21	27	33	40	49	58	69	80	89	89	81

TABLE I *(continued)*

l \ V	+10	15	20	25	30	35	40	45	50	55	60	65	70	75	80	85	90	95	100	105	110	115	120	125	130	+135
220°	60	63	63	65	68	61	48	39	34	30	27	26	28	32	37	38	38	35	29	23	17	12	8	5	1	
215	43	59	62	50	31	17	11	13	17	20	22	24	24	25	28	33	33	29	21	15	9	8	10	10	11	
210	38	55	61	48	28	15	8	9	18	29	44	51	51	48	41	37	30	27	20	12	9	8	7	5	3	2
205	32	46	63	61	50	32	22	30	44	54	58	62	60	58	58	52	40	28	18	14	11	7	4	4	0	
200	34	44	55	57	54	55	65	76	74	63	54	52	54	49	38	27	18	10	6	2						
195	51	60	53	39	35	37	39	35	29	31	35	39	36	29	21	12	5	1								
190	49	56	51	43	41	43	44	42	43	49	53	46	37	25	15	6										
185	43	55	66	77	79	69	57	62	70	73	60	40	27	15	6	0										
180	57	52	50	57	59	60	64	69	65	46	28	16	9	4	2	0										
175	77	85	85	81	79	81	85	68	45	26	12	3														
170	73	76	79	82	76	60	39	21	10	2																
165	99	101	97	80	57	36	20	8	2	0																
160	110	103	83	52	30	14	5	1																		
155	99	74	47	24	10	4	1																			
150	76	43	20	8	2																					
147	60	33	13	5	1																					
145	44	18	6	1																						
140	42	20	10	3																						
135	30	18	10	5	3	1	0																			
130	22	11	4	0																						
125	26	15	12	7	1																					
120	24	10																								
115	18	6																								
110	22	10	6	4	2																					
105	14	5																								
100	24	13	5	0																						
95	14	7	3	0																						
90	18	6																								
85	26	14	7	2																						
80	16	8	5	4	2	1	0																			
75	11	4																								
70	30	12	2																							
65	33	19	9	4	1																					
60	42	19	5																							
55	48	33	18	10	4	2																				
50	91	75	49	26	13	7	2																			
45	88	65	39	22	11	4																				
40	97	80	50	27	13	5	1																			
35	99	91	67	45	23	9	3																			
30	80	83	79	74	70	54	35	22	11	3																
25	78	78	76	79	82	82	71	52	34	21	12	5	1													
20	85	82	76	71	68	67	75	82	82	77	61	33	23	13	7	2										
15	73	76	74	70	67	66	68	76	83	82	75	60	34	16	6	2										
10	59	65	67	68	69	70	65	60	55	56	59	59	52	36	22	12	6	2	0							
5	80	85	84	86	90	90	87	82	77	74	72	69	66	63	57	46	36	25	12	5	0					
0	71	76	81	82	78	69	64	60	59	56	50	44	44	48	49	47	44	38	33	28	20	13	4			
355	53	58	60	64	64	59	52	48	42	40	36	39	43	41	41	45	44	42	36	30	24	19	11	8	4	0
350	63	64	66	65	61	56	53	50	46	41	36	38	35	29	27	30	34	34	31	32	30	23	17	15	10	5
345	62	68	70	65	58	49	40	31	29	21	12	9	13	9	4	0										
340	73	75	75	69	60	52	43	34	24	17	12	7	5	3	2											
335	59	60	58	50	38	26	16	9	5	2	0															
330	69	63	47	31	20	12	6	2	0																	
322	65	47	33	23	17	12	7	4	2	0																

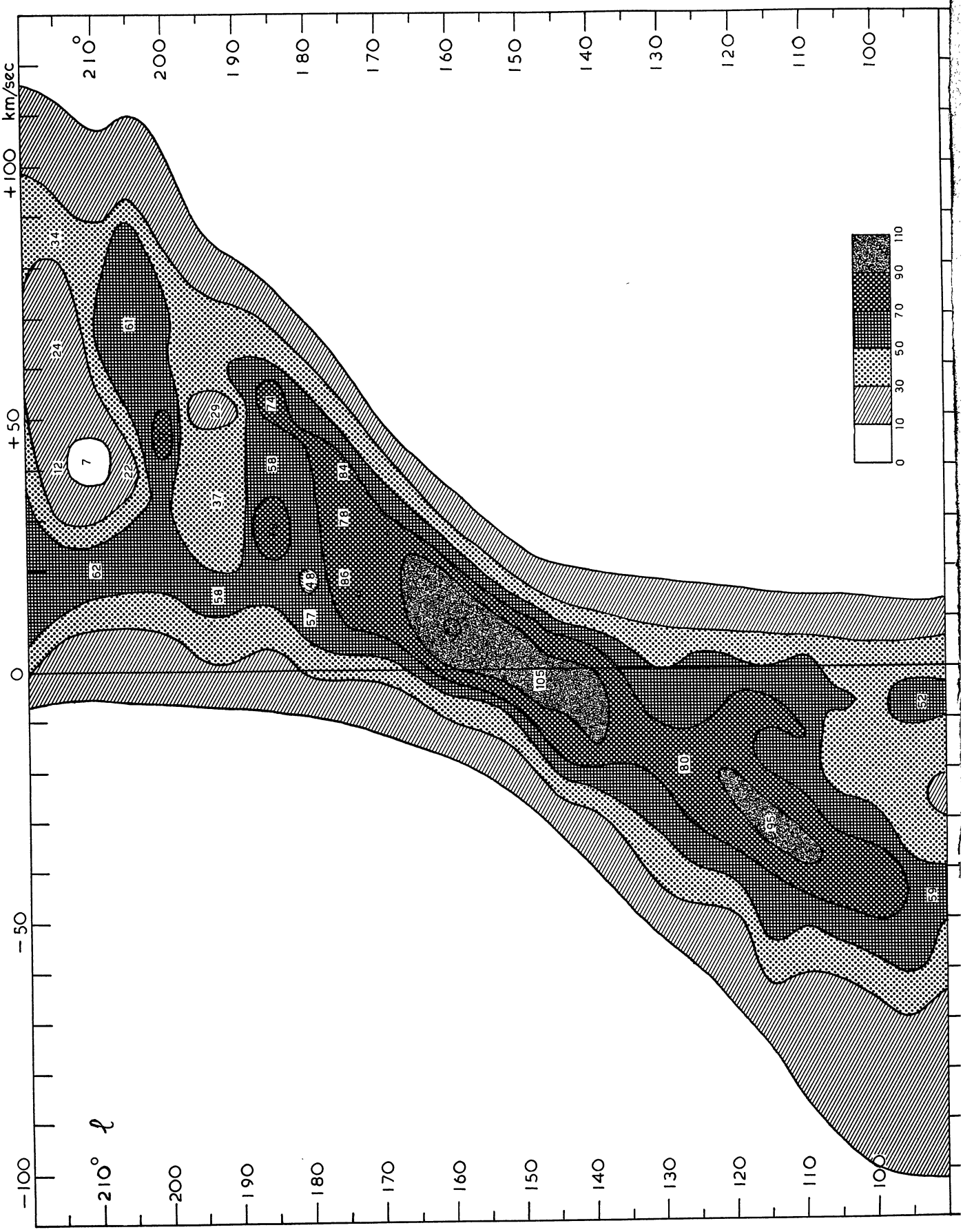

FIGURE 6

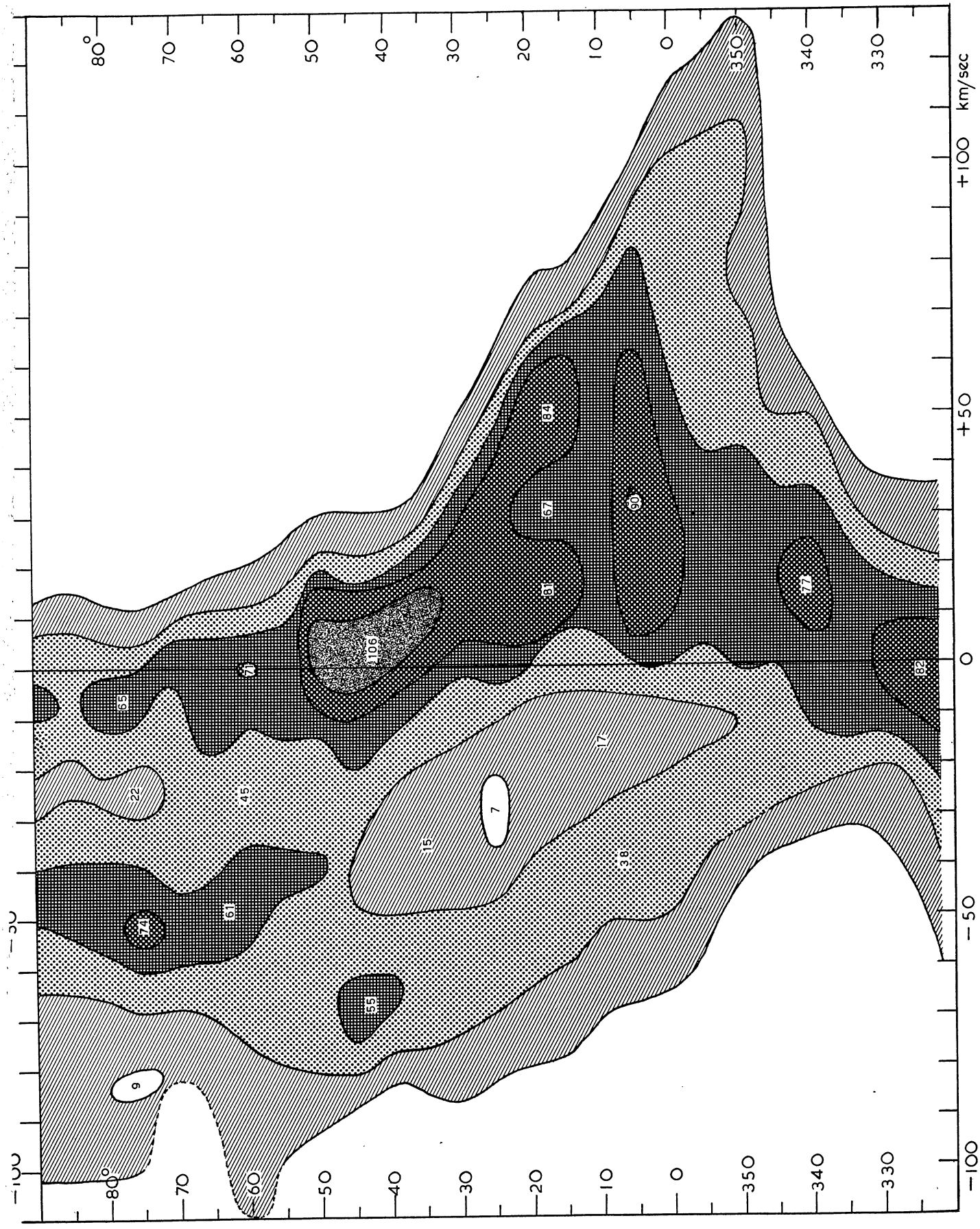

Contour lines of equivalent temperature as function of galactic longitude and velocity. 1 mm = 1 km/sec.

range of 0.8 to 1.2, were determined from a special series of measurements that took about one week. In this series alternative settings were made on a standard strong region ($l = 50°$, $b = 0°$), a standard weak region (the North pole) and on one or two of the measuring points along the galactic equator, each setting lasting for 30 minutes, i.e. giving only a fraction of the line profile.

The final step is the absolute calibration of the common intensity scale. This can only be done by means of the estimated noise figure of the receiver as explained in section 3. On this basis it seems likely that the units of h correspond to 1.0 degree Kelvin in a scale of brightness temperatures. This value will be used in the theoretical discussion (section 16).

8. *Measured line profiles for* $b = 0°$.

The final profiles, 54 in number along the observable part of the galactic equator, are shown together in Figure 5. They have been plotted in such a way that they are oriented as in Figure 3. The right-hand side is the side of high scale reading y, low frequency ν, and positive radial velocity, i.e. by usual astronomical convention a velocity of recession of the observed object with respect to the neighbourhood of the sun. The left-hand side is the side of high frequency and velocity of approach.

The estimated accuracy is of the order of 5 per cent in the strongest intensities and of 1 or 2 km/sec in the velocities, with the possibility of occasional systematic shifts of that same order. More precise measurements are possible with the equipment that has now been developed. Nevertheless, the earlier results are of sufficient interest to give also a complete tabular presentation of the intensity distribution. This is given in Table 1. Interpolation between the values given in the table is not very certain, for the intervals of 5° are twice the beam width, so that important details may have been missed. A smooth interpolation can be made by means of the contour map given in Figure 6.

9. *Some observations outside the galactic plane.*

A systematic investigation of the distribution of intensity in galactic latitude is now being made. The determination of the precise plane of symmetry of the hydrogen radiation, and the location in space of the individual arms, will be possible only after this systematic investigation will have been completed. A small number of incidental measurements outside the galactic plane had been made previous to the new, systematic series. For the present we limit ourselves mainly to a brief description of these tentative early measures.

Recent tracings across the galaxy at frequencies corresponding to the inner part of the Galactic System indicate that between 345° and 10° longitude the plane of symmetry of this inner part lies systematically 1°.5 south of the standard plane adopted in OHLSSON's tables, or 0°.5 south of the galactic plane corresponding to the pole determined by VAN TULDER [1]).

a. *Across the plane at* $l = 327°$: The maximum occurs one degree south of the adopted equator. There is a strong northern extension, so that even at $b = +20°$ the intensity is strong. This region coincides with the dark clouds in Ophiuchus.

b. *Across the plane at* $l = 20°$: The main peak (corresponding to the spiral arm in which the sun is located) is symmetric in latitude, and the intensity falls down to half at $b = \pm 5°$. The fall in the second peak is somewhat sharper. Drift curves (see section 4) for this frequency indicate that the maximum emission near $l = 20°$ occurs at $b = -1°.1 \pm 0°.3$ and near $l = 10°$ at $b = -1°.6 \pm 0°.3$.

c. *Across the plane at* $l = 50°$: The total latitude interval between half-intensity points is 14° for the main peak and between 5° and 6° for the two other peaks. This is in qualitative agreement with the increasing distance of the portions of spiral arms that give rise to these peaks. In this region the maximum intensity is at positive latitude: +0°.5 for the main peak and second peak, but +1°.5 for the third peak, so that this outermost spiral arm seems tilted from the plane of the other ones.

d. *Across the plane at* $l = 80°$: The situation for the main peak seems confused by local clouds. The second peak is centered at $b = -0°.5$ and has a total latitude range of 11° between half-intensity points.

e. *The north pole:* The north pole of 1953 is at $l = 89°.9$, $b = +27°.7$ and is in a known region of weak obscuration. This region has been observed more than forty times in the course of the intensity calibrations referred to in section 7. The line has the central intensity 14 ± 1 in the same scale as used in the preceding sections, a total width between half-power points of 22 km/sec and a central frequency corresponding to −6 km/sec.

f. *Some dark regions in Taurus:* Four points were observed with the following galactic co-ordinates:

Region	l	b	Obscuration	21-cm Intensity
(a)	141°.0	−12°.7	strong	32
(b)	147 .8	−12 .0	weak	43
(c)	126 .3	−20 .0	strong	24
(d)	120 .3	−19 .7	weak	18

Regions (a) and (b) are at about the same latitude; (a) is a small region of exceptionally strong absorption

[1]) *B.A.N.* 9, 315, 1942; No. 353.

(the extra absorption caused by the Taurus nebulae may be estimated from McCuskey's star counts [1]) to average about $2^m.5$ over an area of 2°.5 diameter centered on (a)), while in the comparison region (b) the extra absorption is negligible. If we suppose that the hydrogen is as strongly concentrated in the dark nebula as the dust, an intensity comparable to the maximum intensity in the Milky Way should have been found. We observed only 30% of this intensity. This may mean that in the very dense cloud the hydrogen atoms have mostly combined into molecules. An alternative possibility is that the temperature in the dense cloud would be lower than that in the HI clouds in general.

Regions (c) and (d) are likewise in the same latitude. From the star counts the extra absorption caused by the cloud at (c) may be estimated to average $1^m.0$, while it should be negligible in (d). The observed intensity difference between (c) and (d) is again much smaller than that which should correspond to the difference in absorption. The intensities themselves are no higher than what would be expected to be the average background intensity.

Part II. DATA ADOPTED FOR REDUCTION.

10. *The motion of the sun.*

The following standard values were adopted for the motion of the sun: velocity 20.0 km/sec directed towards $\alpha = 18^h0^m$, $\delta = +30.°0$ (1900), corresponding with $l = 23°.5$, $b = +21°.6$. These standard values correspond closely to the sun's motion relative to the average interstellar medium in its surroundings, as derived from interstellar absorption lines. In a recent new discussion of these interstellar lines Blaauw [2]) gives a velocity of 20.1 km/sec $\pm$0.7 (p.e.) towards $l = 19°.1 \pm 1°.7$, $b = +22°.8 \pm 4°.6$, or $\alpha = 267°.1$, $\delta = +26°.6$. He refers to older results by Plaskett and Pearce, and by Oort, which give a somewhat higher longitude of the apex (22°) and practically the same velocity. From a somewhat different material van Rhijn has likewise derived the sun's velocity with respect to the interstellar clouds [3]). He assumes the apex position found by Plaskett and Pearce [4]) ($l = 22°$, $b = +21°$) and then finds a velocity of 18.4 km/sec $\pm$0.9 (m.e.) from interstellar calcium lines, and 20.2 km/sec $\pm$0.7 (m.e.) from sodium lines.

The solar motion values are confirmed by the proper motions and radial velocities of early B-type stars and other supergiants which, on account of their young age and small velocities may be thought to share the average motion of the medium from which they were formed, while at the same time they cover so large a region of space that local "streams" may have little effect. Recent determinations have been published by Blaauw and van Rhijn. The former finds [5]) from proper motions $\alpha = 275°$, $\delta = +36°$, or $l = 31°$, $b = +20°$; from radial velocities $l = 26°.2 \pm 3°.0$ (p.e.), velocity projected on galactic plane 20.3 km/sec $\pm$1.0 (p.e.). van Rhijn, solving for the velocity only, obtains a value of 20.1 km/sec from *stars* in which interstellar lines had been measured [6]).

A new determination of the solar motion from δ Cephei variables by E. Raimond [7]) yields 21.9 km/sec $\pm$1.9 (m.e.) towards longitude $34° \pm 6°$ (m.e.), latitude +20° ($\alpha = 276°$, $\delta = +39°$). In this solution the Z-component of the solar motion was assumed to be +7.3 km/sec.

The results of the 21-cm line measures, which have been corrected for the standard solar motion cited above, confirm these values to some extent. For one component this is shown by the fact that the line contours in the centre and anticentre are roughly symmetrical around the rest frequency of the line. The significance of this statement is somewhat restricted by the fact that, when these profiles are studied in more detail, we find some asymmetric features, particularly at $l = 145°$ and $l = 327°$. Any local disturbance will have the least influence in that part of the curve where the optical thickness is highest. For the present purpose we have therefore principally confined our attention to these parts of the profiles. Table 2 lists the velocities corresponding to the main maxima in three longitudes opposite the centre and five around the centre. The results were computed by Westerhout

Table 2

l	b	V (km/sec) maximum	V (km/sec) line of symmetry
°	°		
145.0	0	−1.5 (3)	
147.5	0	−0.8 (3)	
150.0	0	+1.5 (4)	
322.8	−1.7	−1.7 (3)	−1.0 (2)
325.8	−1.4	−1.4 (2)	+1.8 (2)
328.3	−1.4	−1.6 (2)	+1.9 (1)
330.8	−1.4	−0.7 (4)	
333.3	−1.5	−1.7 (2)	
40.0	0	+4.0 (4)	
42.5	0	+2.1 (3)	
45.0	0	+1.7 (3)	

[1]) *Ap. J.* **88**, 209, 1938.
[2]) *B.A.N.* **11**, 459, 1952; No. 436.
[3]) *Publ. Kapteyn Lab. Groningen* No. 50, p. 16, 1946.
[4]) *Victoria Publ.* **5**, 196, 1933.
[5]) *B.A.N.* **10**, 28, 1944; No. 363.
[6]) *L.c.*, p. 15.
[7]) *B.A.N.* **12**, 99, 1954; No. 450.

from tracings made in December 1953 and January 1954 with the improved receiver and improved calibration. The numbers of profiles used are indicated between parentheses.

For the directions near the anticentre a fairly reliable estimate can be made, by means of the tracings observed in other longitudes, of the average galactic rotation effect to be expected. This gives — 1.6 km/sec for $l = 145°$ and + 2.4 km/sec for $l = 150°$. The residuals for the three longitudes are thus + 0.1, — 0.8 and — 0.9, or — 0.5 km/sec for the average. The interagreement is very satisfactory, and may be further extended by including the longitudes 140° and 155°. From Figure 5 we can infer that the velocities at these longitudes must also very closely conform to this velocity.

It is difficult to infer anything definite from the profiles near the centre, because these are complicated by the well-known large near-by cloud complex in Ophiuchus, Scorpius and Sagittarius, which apparently causes an asymmetry, and even a dip in several of the line profiles. It is not impossible that the dip is caused by absorption. We have given the velocity corresponding to the highest top as well as the position of the line of symmetry. The latter is particularly uncertain. The average of the two determinations for the three longitudes nearest the centre is practically zero. The results for the centre and anticentre show that the solar motion in this direction does not need any correction.

The contours at $l = 45°$, 42°.5 and 40°, where the optical thickness in the principal maximum again becomes considerable, may be used to check the other galactic component of the solar motion. From three recent tracings at $l = 45°$ we find + 1.7 km/sec for the velocity of the top part, which is fairly broad. The differential rotation for the point of largest optical depth was calculated as + 4.2 km/sec. The velocity remaining after the rotation effect has been removed becomes then — 2.5 km/sec. Similar calculations for 42°.5 and 40° give residuals of — 4.3 and — 4.5 km/sec, respectively. These results indicate that the sun's velocity relative to the rather distant gas clouds in this arm would be about 3.5 km/sec higher than the standard velocity assumed. Part of the residuals may, however, be due to the uncertainty in the correction for differential rotation.

It is to be noted that the above measures also indicate that, at least over large stretches in the general directions of the centre and anticentre, the material has no appreciable systematic motion towards or away from the centre.

In order to facilitate the reduction of the measured velocities to the standard frame of reference described, tables have been constructed which give, for each day of the year and for each 5° longitude, the part of the observed velocities that is due to the earth's orbital motion and to the motion of the sun. The table gives these motions for points on the galactic equator as well as for points in the same declination differing by $+ 60^{min}$ and $- 60^{min}$, respectively, from the right-ascension of the galactic equator.

11. *Galactic co-ordinates used, and adopted longitude of the centre.*

The galactic co-ordinates used are for the equinox of 1900 and are referred to the standard pole at $12^h40^m.0, +28°.0$; the conversion to equatorial co-ordinates was effected with the aid of OHLSSON's tables[1]). In order to avoid confusion galactic longitude will always be counted from the intersection of the 1900 equator with the galactic circle. The galactic co-ordinates of a non-moving star are then fixed quantities, not depending upon the equinox. Galactic co-ordinates so defined, corresponding to a certain azimuth and altitude or right-ascension and declination in 1953, are obtained by reducing α and δ to 1900 and entering OHLSSON's tables with α, δ (1900). This procedure is in agreement with established practice.

It is probable that in future work a correction of at least 1° will have to be applied to the standard pole used by OHLSSON. Such a correction has been indicated by VAN TULDER's work on distant galactic stars, and is also indicated by the present measures. Measures of the continuous radiation near the centre, at 100 and 200 Mc/s (by BOLTON and WESTFOLD, and by ALLEN and GUM, respectively) are likewise in general agreement with VAN TULDER's pole. It is probable that from the 21-cm measures the galactic pole can be determined with considerably better accuracy than from the stellar or radio data heretofore available; but additional observations are required, and we have therefore preferred for the present article to use the standard pole.

The longitude of the centre of the Galactic System can best be determined from objects that are strongly concentrated towards the central region, and whose observed distribution is not too much influenced by absorption. Various determinations have been assembled by one of the authors[2]). A combination of these results yielded $l_c = 327° \pm 1°$ m.e. This value has been adopted in the present article. We prefer not to use the 21-cm measures themselves for a determination of this longitude, as we do not want to assume a priori that the motion of the interstellar matter is exactly circular around the galactic centre. An independent, and very precise determination may be made from measures of the rotation very near the centre. These measures have not yet been completed. Provisional data obtained by WESTERHOUT give $l_c = 328.0$.

[1]) *Lund Annals* No. 3, 1932.
[2]) J. H. OORT, *Ap. J.* **116**, 237, 1952.

12. *Rotation of the Galactic System. The sun's distance from the centre.*

Let for a given point in the galactic plane r = SP (see Figure 7) denote the distance from the sun, $l' = l - 327°$ the angle between the direction of P and that of the galactic centre, R the distance from the centre, and $\omega(R)$ the angular velocity of galactic rotation. A simple geometrical consideration shows that, if the average motion of the medium is everywhere perpendicular to the radius vector from the centre, and if $\omega(R)$ does not depend upon the position angle of this radius vector, the average radial velocity V_g of the medium near P with respect to the average of the medium near the sun is given by the following formula [1])

FIGURE 7

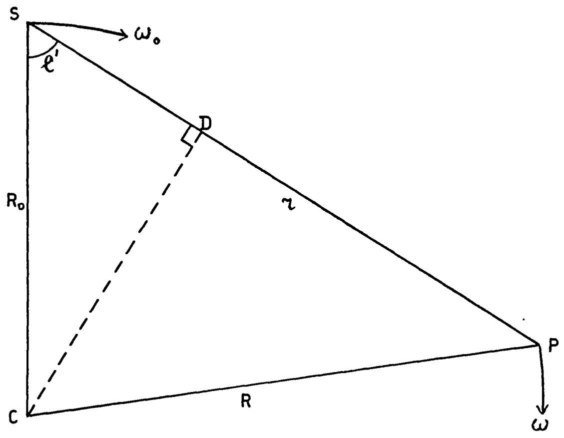

$$V_g = R_0 \{\omega(R) - \omega_0\} \sin l', \qquad (3)$$

where R_0 is the distance from the sun to the centre, and ω_0 the angular velocity near the sun. We shall use kps as unit of distance, and km/sec as unit of velocity.

For $l' < 90°$ the line of sight passes through regions of positive as well as negative velocity. The maximum velocity occurs at the point D closest to the centre C (cf. Figure 7), and near this point the velocity remains nearly constant over a long path. If D is in an arm this should result in a fairly intense radiation sharply dropping to zero at the side of increasing velocities. We see this clearly illustrated by the line profiles between 15° and 30° longitude. It is possible to measure at what velocity (V_{max}) this drop occurs (taking account of the smoothing caused by random motions), and thus to determine by means of (3) the rotational velocity at D, i.e. at a distance $R_m = R_0 \sin l'$ from the centre. This presupposes knowledge of R_0 and ω_0. If A and B are the ordinary constants of differential galactic rotation we have $\omega_0 = A - B$. We have adopted $A = +19.5$, $B = -6.9$ km/sec.kps [2]), which gives $\omega_0 = 26.4$ km/sec.kps.

The most reliable direct determination of the distance to the centre, R_0, is that derived by BAADE from the investigation of RR Lyrae variables in a region of the great star cloud in Sagittarius [3]). The data on magnitudes and absorption have been considerably improved since BAADE's first communication, and he has recently derived a value of 8.16 kps for this distance [4]). The reliability of this determination has been increased by the accurate colour measures of faint stars in some globular clusters by ARP, BAUM and SANDAGE, by which it is possible to connect the absolute magnitude of RR Lyrae variables with that of stars for which it is known from direct methods. According to BAADE these data confirm that the median absolute magnitude is $0^{M}.0$.

A completely independent determination of the distance to the centre has been made from the profiles of the 21-cm line. Consider an interval of R around R_0 that is small enough to assume that ω varies linearly with R. Near the sun

$$d\omega/dR = -2A/R_0, \qquad (4)$$

so that in the interval considered we may write

$$\omega(R) - \omega_0 = -\frac{2A(R - R_0)}{R_0}. \qquad (5)$$

Inserting in (3), and using this formula for the point D (where $R = R_0 \sin l'$), we get the following expression for the maximum velocity observed in a certain direction

$$V_{max} = 2AR_0(1 - \sin l')\sin l'. \qquad (6)$$

This relation enables us to find the product AR_0 from the long-wave edge of the line profile. From the measures at galactic longitudes 15° to 30°, where R_m is still close enough to R_0 to permit the use of (5), and where presumably D is situated within a spiral arm, we have provisionally derived the values of V_{max} and AR_0 shown in Table 3.

TABLE 3

Values of AR_0 derived from limiting velocities.

l	R_m (kps)	SD (kps)	V_{max} (km/sec)	AR_0 (km/sec)
30°	7.31	3.7	+32	165
25	6.95	4.3	+38	147
20	6.55	4.9	+55	171
15	6.09	5.5	+61	160

[1]) This expression was first used by BOTTLINGER, *Veröff. Berlin-Babelsberg* **10**, No. 2, 1933.

[2]) Cf. H. R. MORGAN and J. H. OORT, *B.A.N.* **11**, 379, 1951.

[3]) Cf. *Michigan Publ.* **10**, 16 a.f., 1951.

[4]) Private communication, and stencilled Lecture Notes, Univ. of Michigan Symposium on Astrophysics 1953.

SD is the distance of the corresponding region from the sun. The weighted average of AR_0 is 161 km/sec. With $A = 19.5$ km/sec.kps this gives $R_0 = 8.26$ kps. We have adopted $R_0 = 8.2$ as the average between BAADE's and our determination. With $A - B = \omega_0 = 26.4$ as quoted, this gives 216 km/sec for Θ_0, the velocity of rotation near the sun. The uncertainty of these values is estimated to be between 5 and 10%.

With the aid of these data the angular rotation has been estimated at those longitudes where the data seem to indicate that in the region where the line of sight comes closest to the centre, it passes through a spiral arm. The angular rotations so derived have been plotted as dots in Figure 8. They rest on a very provisional investigation of the line profiles, in which it was not yet possible to include the region inside $R = 3.2$ kps. It is probable from the sudden shrinking of the line profiles when we pass from $l = 350°$ to $l = 345°$ that the density of atomic hydrogen inside $R = 3.2$ kps is much smaller than in the arm which appears between 3.2 and 4.5 kps distance from the centre.

For R larger than R_0 the graph is based on rotational velocities calculated from a very rough model of the Galactic System. The model is in principle the same as that used in *Ap. J.* **116**, 233, 1952, except that the scale was reduced by a factor 0.87 in order to conform to the lower value of the sun's distance from the centre adopted in the present article. A reduction factor of 0.96 was applied to the angular velocities in order to bring the value near the sun into agreement with the value here adopted. Computations with an improved model are now being carried out, and will be published together with the improved discussion of the rotation of the inner parts.

FIGURE 8

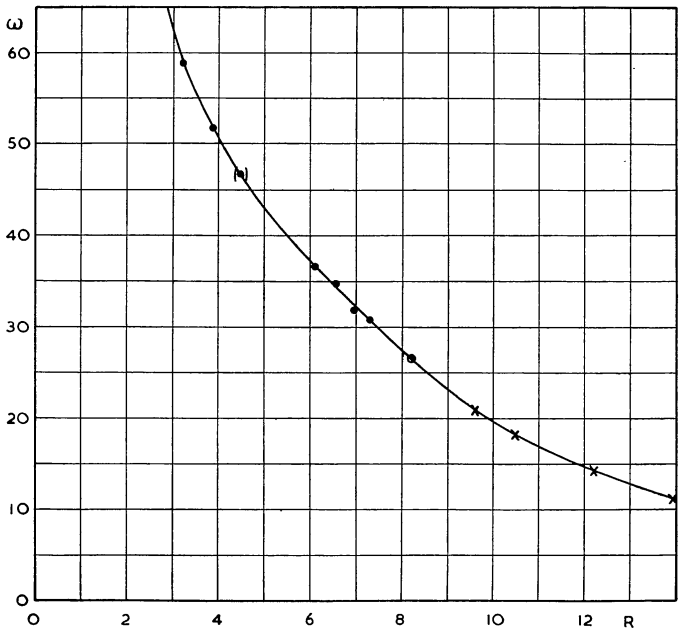

Angular velocity of Galactic System in km/sec.kps as function of distance from the centre in kps.

FIGURE 9

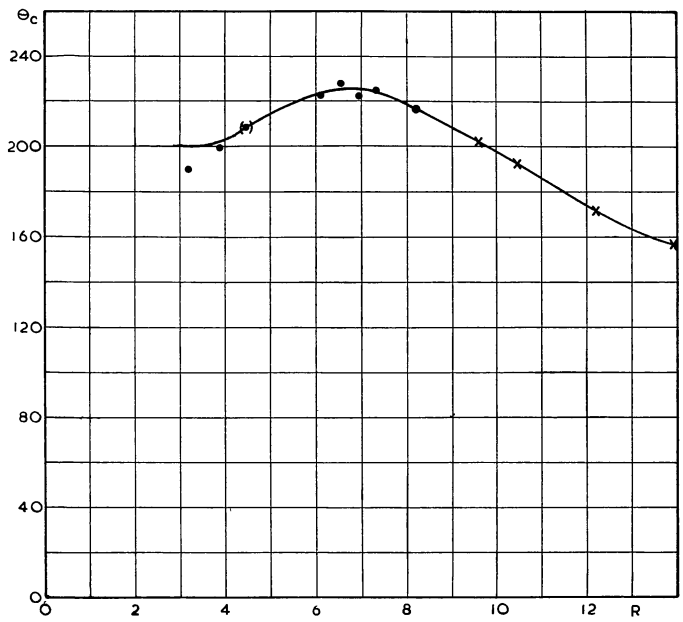

Circular velocity in km/sec as function of distance from the centre in kps.

The dot surrounded by a circle refers to the surroundings of the sun. It corresponds to $R_0 = 8.2$, $\omega_0 = 26.4$.

The linear velocity of rotation $\Theta_c = R\omega(R)$ is shown as a function of R in Figure 9. An extensive investigation on the rotational velocities in the inner part of the Galaxy, based on more recent observations by KWEE and WESTERHOUT, will appear in a forthcoming number of the *B.A.N.*

13. *Deviations from circular motion.*

The preceding section is based on the hypothesis that the systematic motions in the Galactic System are everywhere circular and that, for a given distance from the centre, the circular velocities are the same in all position angles in the galactic plane. It has already been mentioned that the measures made in the directions of the centre and in the opposite direction give some support to this hypothesis (cf. section 10). For the region within 2 kps of the sun it is also supported by the effects of differential rotation in distant stars. These give $l_c = 325° \pm 1°$ m.e.; which means that the *relative* systematic motions in this region are very nearly perpendicular to the direction of the galactic centre. It seemed reasonable, therefore, to use the above hypothesis as a working basis.

On the other hand it is well to point out that the observations show distinctly that here and there deviations from this schematic picture occur. A devia-

tion of this kind is found in the line contour for $l = 145°$, which shows a secondary hump on the side of the negative velocities, by which the line is made much more asymmetrical than it could be on the hypothesis of circular motions. Hump and asymmetry are rather powerful, and the fact that the asymmetry extends over a range of at least 20 km/sec indicates that it is probably caused by something more than just a local cloud. However, at $l = 147°$, the asymmetry has disappeared almost entirely; nor are there any clear signs of it at $l = 140°$. The phenomenon is therefore not of very large scale.

A second indication of deviating motions is found in the longitudes 50° to 60°. As we see from Figure 5, the line profiles in these longitudes extend considerably to positive velocities. The positive wing is of such a shape that it is difficult to ascribe it solely to the dispersion of the cloud velocities in the near-by arm. It indicates that a portion of this arm, situated in the longitude interval 50° to 60°, has a systematic motion away from us superposed on the standard galactic rotation. The amount of this systematic radial velocity is estimated at +3 km/sec for $l = 50°$, +9 km/sec for $l = 55°$, and +4 km/sec at $l = 60°$.

14. *Relation between distance from the sun and radial velocity.*

Once the function $\omega(R)$ as well as the constants R_0 and ω_0 are known, we can derive from (3), for any longitude, the relation between the systematic radial velocity V_g and the distance from the centre R, and therefore also the relation between this radial velocity and the distance from the sun. Plots of V_g against r were prepared for the various longitudes studied, and were used for the conversion of the line profiles into density distributions in section 18.

For values of R differing little from R_0 we can use the expression (5). Inserting this in (3) we have

$$V_g = -2A(R - R_0)\sin l'. \qquad (7)$$

This relation can be used for the ring-shaped region between $R = 6$ and $R = 9$ kps. For small r, $R - R_0 = -r\cos l'$, so that (7) reduces to $V_g = rA\sin 2l'$, which is the usual formula for differential galactic rotation.

A few examples of the relation between V_g and r are shown in Figure 10. In the part inside R_0 there are always two values of r that correspond to the same

FIGURE 10

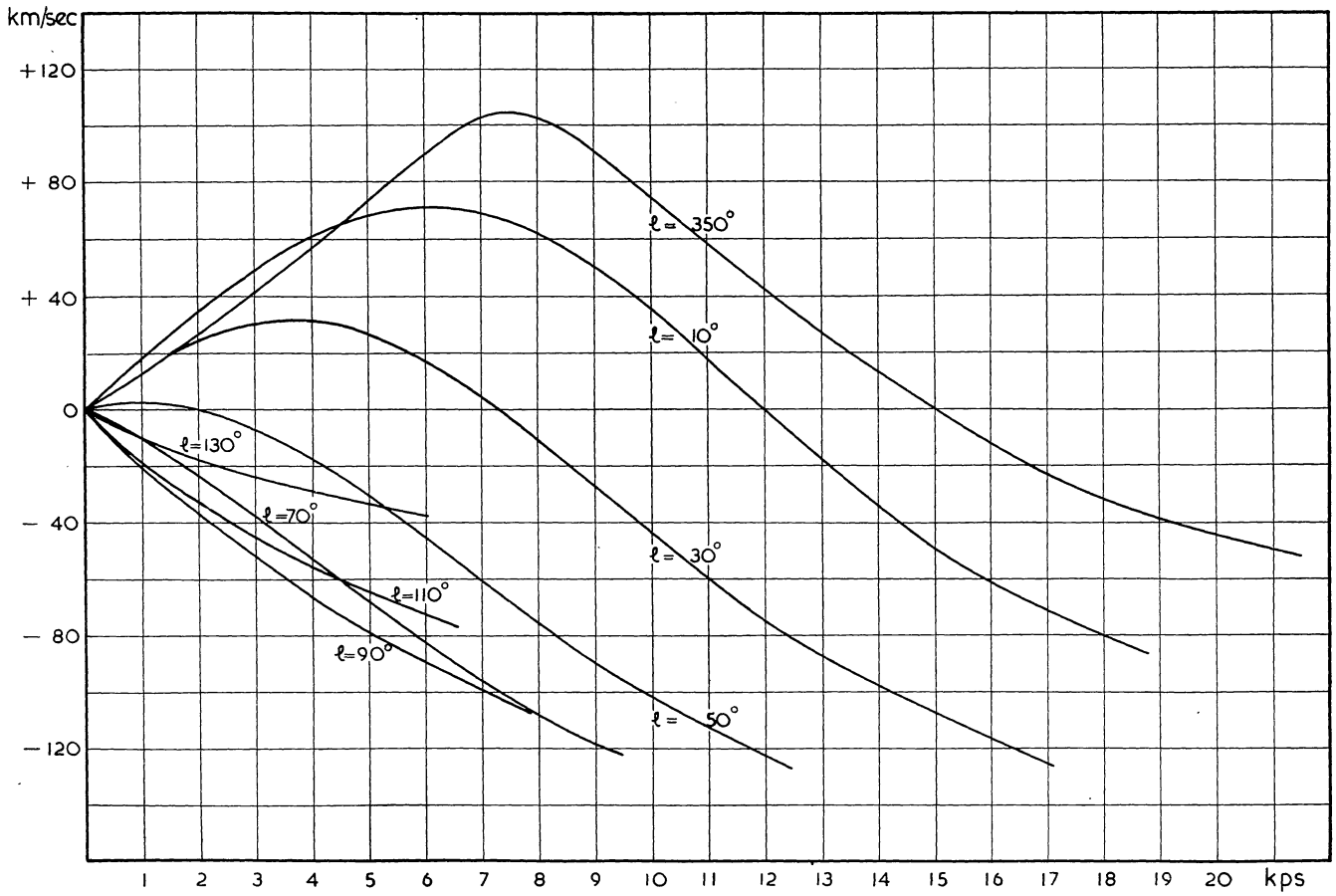

Sample curves of differential galactic rotation in various longitudes as function of distance from the sun.

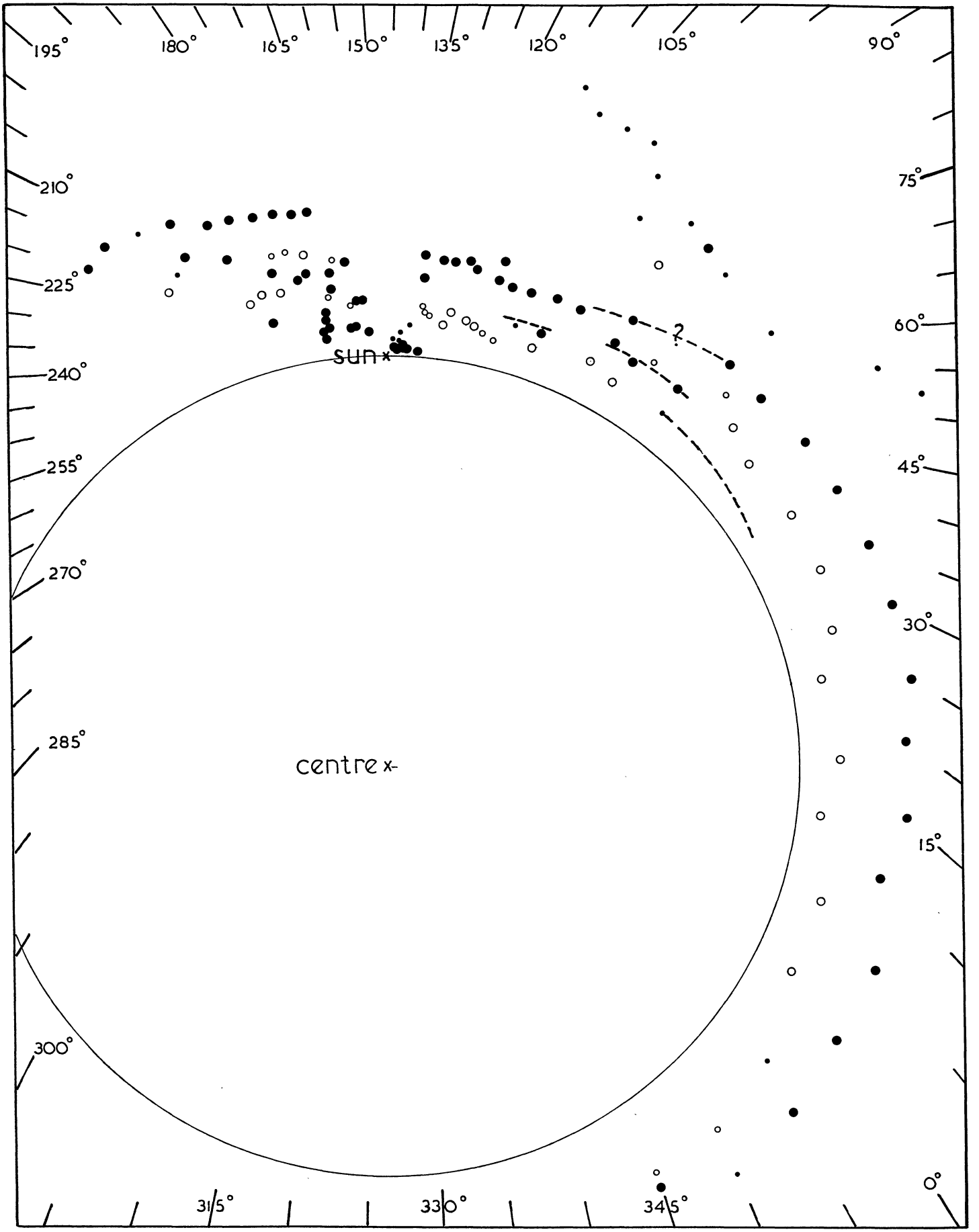

Maxima and minima of hydrogen density in the galactic plane. Numbers indicate galactic longitudes. Principal maxima are shown as large dots, smaller maxima as small dots. Open circles indicate minima. The broken lines indicate continuous sequences of maxima identified on more recent recordings. Scale 1 cm = 1 kps.

value of R, and, therefore, also to the same value of V_g. This makes it much more difficult to obtain the density distribution in this part of the Galactic System. In the present article we have limited ourselves almost completely to a discussion of the outer parts of the system. The inner parts are being reserved for a special investigation.

Part III. INTERPRETATION OF RESULTS.

15. *Geometrical interpretation. Spiral arms.*

With the aid of the graphs described in the preceding section we have determined the positions in space corresponding to the maxima, minima and shoulders in the line profiles. These have been plotted in Figure 11. The large dots refer to maxima of considerable intensity, while small dots represent regions where the hydrogen is concentrated, but with rather lower density. Regions of minimum hydrogen density are shown by open circles, larger circles referring to deep minima. Figure 11 rests wholly on observations obtained before July 1953, except for the interval from 35°—75°, where some results obtained recently with the improved receiver have been used to elucidate the connections between the various arms in this region.

It is evident that the hydrogen is concentrated in relatively narrow lanes separated by regions of much smaller density. We shall see in section 18 that in the latter regions the density is probably negligible. The long stretches of hydrogen are evidently to be identified with "spiral" arms.

The first successful identification of such arms in the Galactic System has been made by W. W. MORGAN and his collaborators at the Yerkes Observatory from the distribution of regions of ionized hydrogen [1]). This investigation was later extended through a study of the space distribution of O associations [2]). The first indication of spiral arms from observations of the 21-cm line was obtained by CHRISTIANSEN and HINDMAN [3]). A comparison of our results with these and other investigations will be given in section 19.

The sun is located in a spiral arm. In all longitudes between 40° and 115° we find in Figure 5 a fairly high maximum near the velocity zero, showing that in these directions the full "arm density" of the hydrogen starts right near the sun, and does not increase upon further penetration into the arm. In the longitudes between 170° and 220° this is quite different. Here the first maximum is situated at some distance from zero, indicating either that the matter is systematically receding from the sun at a rate of about 25 km/sec, or that in these directions the density of hydrogen is quite low at small distances, full spiral-arm densities not being attained until we reach distances from 500 to 1000 parsecs. The latter alternative appears the more probable one. This would indicate that the sun must be situated close to the inner edge of the spiral arm considered. It also indicates that, in our vicinity, this edge is rather strongly inclined with respect to a circle around the galactic centre.

It is convenient to attach names to the various arms that can be distinguished. Ultimately it may be practical to designate the different arms by numbers. In order to provide a provisional means for referring to the various arms already discovered, especially those that are also observable in optical wave lengths, we propose to name the principal arms after conspicuous associations contained in them. After consultation with W. W. MORGAN the following designations are proposed: For the arm passing through the sun: Orion arm; for that passing through h and χ Persei: Perseus arm; and for the first arm encountered when proceeding in the direction of the centre: Sagittarius arm. Being inside the sun's distance from the centre the latter does not appear in our present article. It is conspicuous in the investigation by MORGAN, WHITFORD and CODE by a number of bright associations in the constellation of Sagittarius.

In the longitude interval above 160° the structure is quite complicated. Part of this may be due to a branching of the Orion arm, which is more clearly shown by the arrangement of the associations of early-type supergiants discussed by MORGAN, WHITFORD and CODE.

The Perseus arm is most clearly seen from longitude 50° to 115°. It contains, as one of its most conspicuous features, the rich association of early-type supergiants surrounding the double cluster in Perseus. In longitudes 120° to 130° it is probably present in comparable strength, but more difficult to separate from the Orion arm, due to the smaller differential rotation, combined, probably, with the effect of the branching of the Orion arm. From 135° to 160° the differential rotation is too small for any separation to be possible. The first signs of such separation appear again at $l =$ 170°, where the distant maximum is of considerable strength; it reappears in all higher longitudes up to the limit to which observations can be carried from our latitude. This powerful outer arm may be a continuation of the Perseus arm.

Below 75° longitude another arm becomes visible, about 0.6 kps inside the Perseus arm, and of much the same strength.

The transition from 70° to 50° can be traced much better from the new line profiles that have recently been obtained, which show more detail and are spaced $2\frac{1}{2}$° in longitude. These show that the broad maximum shown in Figure 5 for $l = 65$° consists in

---

[1]) W. W. MORGAN, SHARPLESS and OSTERBROCK, *A. J.* **57**, 3, 1952; also *Sky and Telescope* **11**, 134, 1952.
[2]) W. W. MORGAN, WHITFORD and CODE, *Ap. J.* **118**, 318, 1953.
[3]) *Australian J. Sc. Res.* A **5**, 437, 1952.

reality of two separate maxima, both of which can be followed from 70° to 57°.5 longitude, and continue as the striking maxima observed at $l = 55°$ and 50° in Figure 5. In order to avoid possible wrong interpretation we have indicated by broken lines in Figure 11 the more or less continuous sequences of maxima derived from the new tracings. The separate part inside the Perseus arm ends at 47°.5 ,where there seems to be a break, and a new detached part begins, about ½ kps nearer the centre. This can be followed down to $l = 30°$.

Perhaps the most striking feature of Figure 11 is the strong outer arm seen from $l = 55°$ down to $l = 345°$. Over the entire range between 0° and 55° the arm is separated by a deep and wide minimum from the more inward parts of the system. We shall provisionally refer to this arm as the "distant arm". As we see from the figure, there may well be a continuous transition between this and the Perseus arm. If this is so, the latter would be practically circular over the whole interval from 350° to 125°.

An unexpected, striking feature of the "distant arm" is its great thickness perpendicular to the galactic plane. From a few tentative tracings across the arm at 0°, 10°, 20° and 30° longitude we derive an average thickness of 800 ps between points where the density has become half the maximum density. This is three times the thickness found in our surroundings and in the Perseus arm. The distant arm lies slightly north of the plane of symmetry of the more central part of the Galactic System.

Between $l = 60°$ and 120° the line profiles clearly show the existence of a third, more distant arm. The much improved records obtained since November 1953, which in general have not yet been used for the present article, show this outer arm much more clearly, and confirm that it is a continuous arm of considerable width, also in a direction perpendicular to the galactic plane. Its thickness in the latter direction may be estimated as between 3 and 4 times that of the nearer arms. The arm lies somewhat north of the standard galactic plane. On these new records it can be traced also at lower longitudes, mostly in the form of a slowly decreasing density, extending some two or three kps beyond the large Perseus arm. At 35° and 47°.5 it can be distinguished as an actual concentration.

The density in this outer arm is only about 1/10 of that in the Orion and Perseus arms. We shall provisionally refer to it as the "thin outer arm". It is probably the outermost continuous arm of the part of the Galactic System that has been surveyed. The determination of its position is rather uncertain because it depends on a considerable extrapolation of the $\omega(R)$-curve.

If it is actually one continuous arm it would be strongly inclined with respect to a circle around the galactic centre; a feature that was also shown in the near-by arm discussed by MORGAN and his collaborators. These phenomena indicate that the relation between the directions of galactic rotation and of the winding of the arms is such that the arms are trailing.

On the whole the principal arms appear to deviate but little from circles. This applies not only to the Perseus arm and the "distant arm", but also to an arm between 345° and 30° longitude, just inside the circle with radius R_0, which has recently been found by SCHMIDT. This arm may be a continuation of the Orion arm.

Judging from the inclination of the arms the Galactic System may be intermediate between an Sa and an Sb spiral, possibly resembling a system like NGC 488, or NGC 4594 [1]).

The investigation of the density distribution in the part of the Galactic System that is closer to the centre than the sun is being made partly from tracings perpendicular to the Milky Way at various fixed frequencies. These will be discussed in another article.

At present we will only point to one striking feature concerning the central region. In Figure 5 a sudden change may be seen to take place between 350° and 345° longitude, in the right-hand part of the line profile. Proceeding from 0° to 355° and 350° the profiles become gradually broader, but at 345° a large fraction of the right-hand part has suddenly disappeared. From improved records it appears that it does not disappear entirely, but is present in all longitudes down to 330° as a very low, long toe, extending even further than the profile at 350°. A discussion of these profiles will be given in a subsequent article. The interpretation is complicated, but the outspoken decrease in intensity may be taken as an indication that the density of atomic hydrogen diminishes for $R < 3$ kps.

16. *Temperature and optical depth.*

Let $n_m(V,r)dV$ be the number of hydrogen atoms per cm³ in the upper level at a distance r and with radial velocities between V and $V + dV$. Let $N_m(V)dV$ be the number of atoms in the same level and in the same velocity range in a column of cross-section 1 cm² along the entire line of sight. Then

$$N_m(V) = \int_0^\infty n_m(V,r)\,dr.$$

The same notation with index n will refer to the lower level.

The radiation received per cm² per sec per unit solid angle in a frequency interval $d\nu$ from an optically thin layer is

$$I(\nu)\,d\nu = \frac{h\nu}{4\pi} A_{mn} N_m(V)\,dV. \qquad (8)$$

[1]) For the arms in NGC 4594 see LINDBLAD, *Publ. A.S.P.* **63**, 133, 1951.

Here A_{mn} is the transition probability for spontaneous emission and $dV = \frac{c}{\nu} d\nu$. The 21-cm line has [1])

$A_{mn} = \frac{64\pi^4 \nu^3}{3h\ c^3} \beta_o^2 = 2.84 \times 10^{-15}$ sec^{-1}, where β_o is the Bohr magneton. The atomic absorption coefficient $\varkappa(\nu)$ (cm^2) is related to the transition probability for absorption, B_{nm}, by the well known relation:

$$\int \varkappa(\nu)\, d\nu = B_{nm} \frac{h\nu}{4\pi}.$$

Upon the assumption that Doppler effect is the dominant effect of line broadening, this relation leads to the following expression for the absorption coefficient per unit length:

$$k(\nu) = n_n(V,r)\, B_{nm} \frac{hc}{4\pi}. \qquad (9)$$

In the radio (or classical) domain the true absorption is largely compensated by the stimulated emission. The difference is the effective absorption coefficient:

$$k'(\nu) = \frac{h\nu}{kT} \times k(\nu). \qquad (10)$$

Here T is the excitation temperature defined by

$$\frac{n_m}{n_n} = \frac{g_m}{g_n} e^{-h\nu/kT} \approx \frac{g_m}{g_n}\left(1 - \frac{h\nu}{kT}\right).$$

PURCELL and others [2]) have shown that this excitation temperature is made equal to the kinetic temperature in the neutral hydrogen clouds by means of the highly effective process of electron exchange during atom-atom encounters. Another process, that would have had the same effect, was explored by WOUTHUYSEN [3]) but may be shown to be ineffective due to absorption of Lyman alpha quanta by interstellar dust. The temperature found below is 110° so that $h\nu/kT = 0.0006$, which is small enough for the usual approximations for the radio domain to be permitted.

Combining the preceding formulae with the relation

$$B_{nm} = \frac{g_m}{g_n} \frac{c^2}{2h\nu^3} A_{mn},$$

we obtain the optical depth of the entire column in a certain direction

$$\tau(\nu) = \int_o^\infty k'(\nu)\, dr = N_n(V)\, A_{mn} \frac{g_m}{g_n} \frac{c^3}{8\pi\nu^3} \frac{h\nu}{kT}. \qquad (11)$$

Inserting the following numerical values $\nu = 1.4204056 \times 10^9$, $c/\nu = \lambda = 21.105$, $h\nu/k = 6.813 \times 10^{-2}$, $g_m/g_n = 3$ (the upper level being triple), $A_{mn} = 2.84 \times 10^{-15}$, and introducing the total number of hydrogen atoms in the ground state, N, instead of N_n ($N = 4N_n$), we obtain

$$N(V) = 1.835 \times 10^{13}\, T\tau(\nu). \qquad (12)$$

The intensity received from this direction is

$$I(\nu) = I_o(\nu) \times (1 - e^{-\tau(\nu)}), \qquad (13)$$

where $I_o(\nu)$ is the intensity of a black body, which is $I_o = \frac{2\nu^2}{c^2} kT$ according to the law of Rayleigh-Jeans. Equation (13), when combined with (11), reduces to (8) in the limit of small τ.

Estimates of I_o and of the absorption coefficient have been made in the following ways.

a) By a comparison of the maximum intensity of the Orion arm when observed in longitudes 80° to 100° and 40° to 45°, respectively. In the first interval the line of sight passes through this arm under a large angle, while at the same time, as may be seen from Figure 5, the arms are well separated. In the second interval the line of sight lies inside the arm over a considerable range of distance. That this is so, is shown clearly by the plot of O associations published by MORGAN, WHITFORD and CODE [4]), where the arm is observed up to 2.3 kps. For the following we shall assume that the arm continues beyond this distance.

In the direction of 45° longitude the maximum radial velocity due to differential rotation is +7 km/sec. The velocity becomes zero at a distance of 4.2 kps. Over this whole stretch the differential rotation effects are small compared to those of random motions. If we denote by τ_4 the optical thickness in the centre of the line at $l = 45°$, we see that τ_4 is equivalent to 4.2 kps of arm density with negligible differential rotation effects. Similarly we call the optical thickness in the centre of the first maximum in longitudes 80°–100°, τ_3. Here we traverse an effective thickness of about 0.7 kps of the Orion arm (cf. section 18). The differential rotation increases to about −13 km/sec over this interval, which must have made the spread in velocity greater than it would have been without rotation. Very roughly, we estimate that under these circumstances the maximum intensity is the same as that which would have been observed from a stretch of 0.6 kps without differential rotation. So τ_3 is equivalent with 0.6 kps of arm density without rotation. This estimate is uncertain, but the resulting value of I_o is hardly influenced by errors up to 20% in this length. The ratio of the optical thicknesses in the two cases is thus $\tau_4/\tau_3 = 7$.

In the direction $l = 40°$ the maximum galactic rotation effect is +13.5 km/sec; it becomes zero at a

[1]) P. WILD, *Ap. J.* **115**, 206, 1952.
[2]) H. I. EWEN and E. M. PURCELL, *Nature* **168**, 356, 1951; R. H. DICKE, E. M. PURCELL and J. WITTKE, Paper at the Radio Astronomy conference in Washington, D.C., Jan. 1954.
[3]) S. WOUTHUYSEN, *Physica* **18**, 75, 1952.
[4]) *Ap. J.* **118**, 318, 1953.

distance of 4.8 kps. In this case the average effect of differential rotation over this stretch will be of the same order as that over the effective thickness of 0.7 kps of the arm in the directions 80° to 100°, and the ratio of the two optical thicknesses τ'_4/τ'_3 will in this case be roughly 4.8/0.7, or again 7.

If we denote by I_3 and I_4 the average maximum intensity in the Orion arm at 80° to 100° and 40° to 45° longitude, respectively, we have $I_3 = 51$ and $I_4 = 105$. The following relations should be fulfilled:

$$\frac{I_3}{I_4} = 0.49 = \frac{1 - e^{-\tau_3}}{1 - e^{-\tau_4}}$$

$$\tau_4 = 7\,\tau_3.$$

These give

$$\tau_3 = 0.65, \qquad \tau_4 = 4.6.$$

From I_4 and τ_4 we find by means of (13) $I_o = 106$. From τ_4 and the length of 4.2 kps over which at $l = 45°$ the differential rotation is small, we find that the average absorption coefficient in the dense part of the arm is 0.91 kps^{-1} in the case of negligible galactic rotation effects; this is for observations in the centre of the line, with a band width of 8.4 km/sec.

b) We can make another estimate of I_o and of the absorption coefficient by comparing the maximum intensity I_1 in the longitudes 140° to 155° with the average maximum I_2 of the two principal arms observed in the longitudes 80° to 100°. For the former we find $I_1 = 105$, while $I_2 = 57$. In the interval 140° to 155° the effects of differential rotation may be neglected. From the line contours observed in other longitudes, and from the general distribution of the hydrogen derived from these, we estimate that in the general direction of the anticentre we have a layer of hydrogen equivalent to about 2.5 arms of a thickness like the two main arms observed at 80° to 100°. In comparing the maximum intensities in the two directions we must further take account of the fact that in the latter direction the differential rotation has considerably widened the profile for each arm. Within an arm the average deviation of this effect from the mean is estimated to be about 8.5 km/sec. This is of the same order as the average random velocity so that, roughly, the observed spread in velocity within an arm must be 1.4 times larger than in a case of negligible rotation; the optical thickness will have decreased by the same factor. The ratio of the optical thicknesses, τ_1/τ_2, will therefore be 1.4×2.5, or 3.5. Combining this with the ratio of the maximum intensities $I_2/I_1 = 57/105 = 0.54$, we find

$$\tau_1 = 2.4, \quad \tau_2 = 0.68.$$

From I_1 and τ_1 we derive $I_o = 116$. From τ_1 and the estimate of 2.5 major arms we find that without galactic rotation the optical thickness per major arm becomes 0.96. As the effective thickness of a major arm may be roughly estimated as 1.0 kps, the absorption coefficient is 0.96 kps^{-1}.

c) A third estimate of the absorption coefficient may be made from the way in which the intensity of the line decreases with increasing latitude. This method has previously been used by MULLER and OORT [1]) and by WILD [2]).

VAN RHIJN has discussed the thickness of the galactic layer of gas [3]) and dust [4]). He finds that the variation of the average density with distance from the galactic plane can be represented by

$$\Delta(z) = \Delta(0)\, e^{-q|z|}, \qquad (14)$$

where z is the distance above the galactic plane in parsecs. Half the equivalent thickness is then $1/q$. The average distance from the galactic plane is also $1/q$. From the interstellar absorption lines VAN RHIJN derives $1/q = 120$ ps; from the colour excesses he finds $1/q = 123$ ps.

Once this effective thickness is known, we can use the intensities observed outside the Milky Way to determine the absorption coefficient. A practical difficulty is the enormous irregularity in the distribution of interstellar material, the influence of which becomes greatly enhanced when we observe in higher latitudes. Our own observations in these latitudes are still too restricted to form a significant average. However, extensive measures of the peak intensity of the 21-cm line have been made by CHRISTIANSEN and HINDMAN [5]). A rough average of their peak intensities at $b = \pm 10°$ for the longitude intervals $40° - 74°$, $310° - 344°$ and $130° - 164°$, where the differential rotation is negligible, gives 11.0. The peak intensity around the anticentre and near $l = 40°$ is about 22. Assuming an average optical thickness of 3 in these directions, the intensity for infinite optical thickness would be 23, and the intensity at $b = 10°$ would correspond to $\tau = 0.65$. This is for a layer of $\frac{120}{\sin 10°} = 690$ ps effective thickness. The absorption coefficient is thus found to be $0.65/0.69 = 0.94$ kps^{-1}. The observations were made with a band width of 10.5 km/sec. A factor 1.06 would be required to reduce to a band width of 8.4 km/sec as used in our own survey. For this latter band width the absorption coefficient would then become 1.00 kps^{-1}.

In view of the great uncertainties the agreement of the three more or less independent results for the mean absorption coefficient in the Orion arm is quite

[1]) *Nature* **168**, 358, 1951.
[2]) *Ap. J.* **115**, 206, 1952.
[3]) *Publ. Kapteyn Lab. Groningen*, No. 50, pp. 10-11, 1946.
[4]) *Publ. Kapteyn Lab. Groningen*, No. 53, p. 9, 1949.
[5]) *Australian J. Sc. Res.* A **5**, 437, 1952.

satisfactory. Giving double weight to the first estimate the average becomes 0.95 kps^{-1}. This is for a band width of 8.4 km/sec. Assuming an average random radial velocity of 8 km/sec the reduction factor to zero band width is found to be 1.27. For zero band width the absorption coefficient would thus be 1.20 kps^{-1}.

We have found in section 7 that one unit in our intensity scale corresponds to 1°.0 in brightness temperature. The weighted average of the values of I_0 derived from the data a) and b) above may be taken as 110, giving $T = 110°$ *). This may be compared to the theoretical predictions of the temperature of interstellar clouds, by SPITZER and his co-workers. SPITZER and SAVEDOFF [1]) arrive at a value of about 60° K for the equilibrium temperature of the electrons in HI regions. This is rather lower than the value derived from the present observations. The difference does not appear too serious, in view of the uncertainty in several of the factors which determine the theoretical value.

In the discussions of this section we have tacitly assumed that the temperature of the HI regions is everywhere the same. In reality there is likely to be considerable variation. If the line of sight passes through many layers of different temperatures that are each optically thin, the integration that led to (13) in the isothermal case is replaced by one in which $I_0(\nu)$ is the black-body intensity corresponding to the harmonic mean temperature. In order to explain the relatively high temperature found it remains necessary, therefore, to suppose that the *major* part of the hydrogen atoms have a temperature that is at least twice that estimated by SPITZER and SAVEDOFF.

So far we have neglected the *continuous radiation*. This can be derived from recent measurements by WESTERHOUT with our equipment at 1420 Mc/s. He finds a temperature of $33° \pm 2°$ for the direction of the centre. At 335° he finds a temperature of 16°. The maximum at the centre appears to be remarkably sharp. Beyond 335° the temperature drops slowly with increasing longitude, reaching about 8° at $l = 15°$. It becomes very small for longitudes above 30°. The variation with longitude corresponds roughly with the measurements of the thin galactic layer made by SCHEUER and RYLE at 210 Mc/s [2]). The peak value is of the same order as that measured by PIDDINGTON and MINNETT at 1210 Mc/s [3]).

The intensity of the emission line at a given frequency comes from atoms in one, or two, fairly narrow distance intervals. We have to consider how the measured intensity is influenced by the continuous radiation from sources in front of, and from sources behind the hydrogen atoms. In the first case the continuous radiation will simply be added to the line intensity as well as to the comparison intensity, and will have no effect on the observed difference. The radiation from sources *behind* the hydrogen atoms will be reduced by a factor $e^{-\tau}$, if τ is the optical thickness of the layer of hydrogen atoms at the frequency considered. Let r be the distance of these hydrogen atoms. Let, further, $I_{c,r}$ be the unreduced intensity of the continuous radiation from sources beyond r; then the intensity actually observed in the differential measurements is

$$I = I_0 (1 - e^{-\tau}) + I_{c,r} e^{-\tau} - I_{c,r}, \qquad (15)$$

where I_0 has the same meaning as above. Hence,

$$\tau = -\ln\left(1 - \frac{I}{I_0 - I_{c,r}}\right). \qquad (16)$$

In this case, therefore, I_0 in (13) has to be replaced by $I_0 - I_{c,r}$.

When we consider the central intensity at $l = 327°$ we are dealing with a case in which practically all the continuous radiation comes from sources more distant than the atoms responsible for the line emission. If, as seems probable, the optical thickness in the line is considerable, the measured temperature should be increased by the brightness temperature of the continuous radiation, or by about 33°, in order to find the excitation temperature of the hydrogen atoms. The observed temperature was 80°, so that the actual temperature becomes 113°. It is interesting that this is very near the temperature of 110° estimated above for the outer arms. The difference is no larger than may be caused by the uncertainty in the estimate of the continuous radiation.

In the other parts of the line at $l = 327°$ the correction becomes more complicated, and will not here be discussed.

In other longitudes the corrections to be applied at a certain frequency can only be estimated after it has been determined what fraction of the observed line radiation comes from each of the two distance intervals concerned. At present it is only near the extreme positive velocities that we have some knowledge about the distance distribution, as the atoms concerned must all lie in the central region. Supposing that in this case half of the sources of continuous radiation would be behind the hydrogen atoms considered, and the other half in front, we may derive the optical thickness from (16), substituting $\frac{1}{2} I_c$ for $I_{c,r}$. For the

*) Note added in proof.
More careful corrections for antenna pattern combined with measurements slightly off the standard galactic equator around the anticentre and at $l = 42°.5$ have indicated a somewhat higher temperature, of around 125°.

[1]) *Ap. J.* **111**, 593, 1950.
[2]) *M.N.* **113**, 3, 1953.
[3]) *Australian J. Sc. Res.* A **4**, 459, 1951.

distant arm observed at negative velocities, the corrections would be negligible.

Finally, we may conclude that on the whole there is no evidence in the present observations of large-scale variations in the average temperature of the HI regions.

17. *Correction for random cloud velocities.*

The distribution of the velocities of interstellar clouds has recently been studied by various authors [1]). All agree that the frequency of high velocities is strikingly greater than would correspond to a Gaussian distribution. We shall tentatively assume that the random radial velocities, v, are distributed as

$$\frac{1}{2\eta} e^{-|v|/\eta}, \qquad (17)$$

where η is the average without regard to sign of the random radial velocities; $\frac{1}{2\eta}$ is a normalizing factor, chosen such that the integral of (17) over all velocities, positive and negative, is unity. This distribution function was suggested in BLAAUW's discussion of the interstellar absorption lines. It also appears to fit reasonably well the present observations of the 21-cm line. For η BLAAUW found 5 km/sec for stars within 500 ps, and 8.2 km/sec for stars between 500 and 900 ps. The latter value agrees fairly with the velocity dispersion found by SPITZER and others from the curve of growth of the absorption lines. SPITZER [2]) deduced a dispersion of 9 km/sec in this way.

An independent determination of the velocity dispersion in the direction perpendicular to the galactic plane may be obtained from the observed density distribution in this direction, in combination with values of $K(z)$ derived from other data[3]). Assuming for the velocities Z in the direction perpendicular to the galactic plane a distribution like (17) we find density distributions as shown in Table 4 under "computed". These may be compared with the distribution inferred from observations. For this we have used VAN RHIJN's formula, given under (14) in the present article, taking $1/q = 122$ ps. The density near the galactic plane has been put equal to 1. We see that the best fit is obtained for $\eta = |\overline{Z}| = 10$ km/sec. The agreement with VAN RHIJN's densities is as good as might be expected. It is quite possible, of course, that the velocity distribution in this direction is different from that in the other co-ordinates; also, it will probably change with increasing z. But, though the evidence is limited, it confirms the general amount of random motion found from the multiple interstellar absorption lines.

TABLE 4

Observed and computed distribution of interstellar matter perpendicular to the galactic plane.

z (ps)	observed	computed	
		$\eta = 8.2$	$\eta = 10.0$
0	1.00	1.00	1.00
50	.66	.80	.82
100	.44	.32	.39
150	.29	.17	.23
200	.19	.12	.17
300	.08	.04	.06
400	.04	.03	.05

The most direct and most valuable information may be obtained from observations of the 21-cm line itself, if this is observed with a smaller band width and, preferably, better angular resolving power than used in the present investigation, in directions where the effects of galactic rotation are small. Such observations have, however, not yet been made. The band width used is such that it smears out most of the individual cloud structure. For an investigation like the present one, concerned with the large-scale features of the distribution, this is no disadvantage.

The line profiles obtained can still be used to determine the general distribution of random motions. For this purpose we consider the longitudes 65° to 130°. In these directions the differential rotation is negative. The positive tails of the line profiles must therefore be due to the deviations from circular motion, and an investigation of these tails will yield a determination of η. A study of the average profiles in these directions gave $\eta = 8.5$ km/sec, with fairly great accuracy. This value is in excellent agreement with the average velocities derived by BLAAUW and by SPITZER, while it agrees well enough with the value of $|\overline{Z}|$ found above. The method by which this result for η was derived will be indicated below, and is fully illustrated in section 18. In the longitudes 170° to 220° the same method cannot be used, because it is apparent that in these directions the interstellar density just beyond the sun is small, becoming large only at distances of the order of 1 kps.

Another estimate may, however, be obtained from the profiles near the anticentre. We shall consider the average of the profiles at 147° and 150°; the one at 145° is less suitable because it is distorted by local effects (section 13). We assume again $\tau = 2.5$ in the centre of the line (as on p. 140). Using the velocity law (17) the best representation of the observed curve

[1]) F. L. WHIPPLE, *Centennial Symposia*, Harvard Obs., 1948; A. BLAAUW, *B.A.N.* **11**, 459, (No. 436), 1952; L. SEARLE, *Ap.J.* **116**, 650, 1952; A. SCHLÜTER, H. SCHMIDT and P. STUMPFF, *Zs. f. Ap.* **33**, 194, 1953.

[2]) *Ap.J.* **108**, 276, 1948.

[3]) *B.A.N.* **6**, 249, 1932.

is obtained with $\eta = 8.3$ km/sec. Figure 12 shows the comparison of the line profile so computed with the observed profile. In the computed curve account has been taken of the flattening of the sharp maximum due to the band width of the receiver. In the other parts of the curve the effect of the band width is negligible. The agreement is not perfect, but sufficient to show that in these directions also the mean random velocity is about 8.5 km/sec.

FIGURE 12

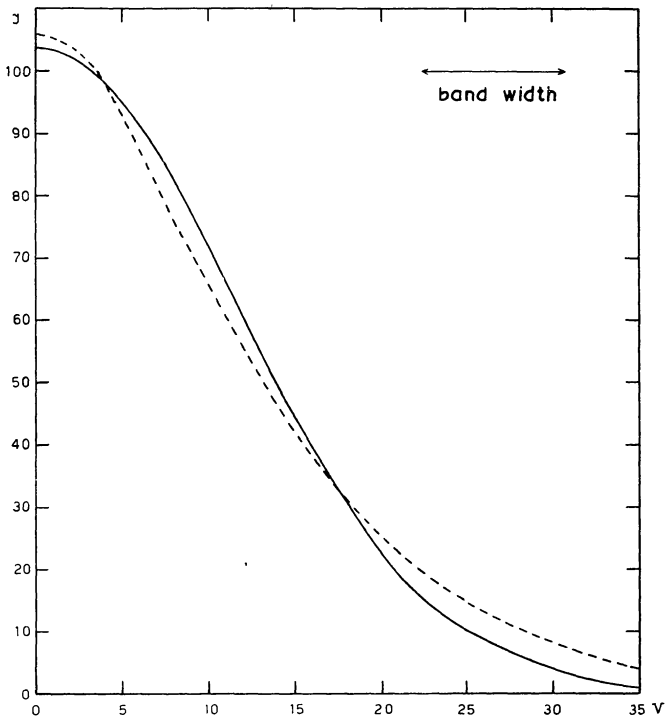

Line profile at 147° and 150° longitude. The full-drawn curve gives the average observed profile, the broken curve is the profile computed on the assumption of an optical depth of 2.5 at the centre of the line, and an average random radial velocity of the clouds of 8.3 km/sec. Abscissae are velocities in km/sec.

It should not be supposed, however, that the distribution of random motions is everywhere the same. The actual line profiles show evidence of considerable local variations. So far as possible these have been taken into account.

If we want to determine the density distribution of the hydrogen atoms observed in a given direction, the effect of the random motions must first be eliminated.

In the direction considered, let $n_H(r)$ be the density of hydrogen atoms. Let, further, V_g be the radial component of the differential galactic rotation at a distance r. Then, if there were no random motions, the number of hydrogen atoms in a column of 1 cm² cross-section and in a unit interval of V_g, would be equal to

$$\mathfrak{N}(V_g) = \frac{n_H(r)}{dV_g/dr}. \qquad (18)$$

The actual velocity distribution will be smeared out by random motions. If the random radial velocities v are supposed to be distributed according to (17), the observed velocity distribution is given by

$$N(V) = \frac{1}{2\eta}\int_{-\infty}^{+\infty} \mathfrak{N}(V_g)\, e^{-|V-V_g|/\eta}\, dV_g. \qquad (19)$$

The integral may formally be extended from $-\infty$ to $+\infty$, as $\mathfrak{N}(V_g)$ is zero below a minimum value and beyond a maximum value of V_g. The determination of $\mathfrak{N}(V_g)$ from the observed function $N(V)$ requires a method for solving this integral equation. A well-known approximate solution for a kernel of arbitrary form is

$$\mathfrak{N}(V) = N(V) - C\frac{d^2N}{dV^2}, \qquad (20)$$

where C is a constant. The constant C may be determined by means of Taylor expansion of $\mathfrak{N}(V_g)$ in powers of $v = V - V_g$ and integration by terms. This method has been applied in the case of a Gaussian error law [1]) and a rectangular smearing function [2]); it gives $C = \eta^2$ in the present case. It is a fortunate accident, however, that the one form of the kernel for which (20) is the exact solution of the integral equation is exactly the distribution function (17). This can be proven by Fourier transforms or, more directly, by differentiation of (19).

In practice it is convenient to use N in tabular form. If Δ is the tabular interval, (20) can then be written

$$\mathfrak{N}(V) - N(V) = -(\eta/\Delta)^2 \times \text{second difference of } N. \qquad (21)$$

In the present case Δ has generally been taken equal to 5 of the units originally used in the reduction of the observations, or 3.59 km/sec. In several cases the results have been checked by means of the rigourous formula (19). It invariably turned out that the approximation given by (21) was almost sufficient.

$N(V)$ can be computed from (13) and (12), inserting $T = 110$. Values of dV_g/dr have been calculated by means of the adopted function $\omega(R)$, which gives also the relation between V_g and r. We can then derive $\mathfrak{N}$ with aid of (21), and compute $n_H(r)$ from (18).

Sample curves of the relation between V_g and r have been given in Figure 10. Figure 13 shows for the same longitudes the values of dV_g/dr.

An example of the effect of the reduction of the intensities to optical depths, and of the correction for the random motions is given in Figure 14. The heavy line represents the measured line profile; the intensity scale as indicated on the left-hand side is the same as

[1]) A. S. EDDINGTON, *M.N.* **73**, 359, 1913; **100**, 354, 1940.
[2]) Lord RAYLEIGH, *Scient. Papers* **1**, 135, 1871.

FIGURE 13

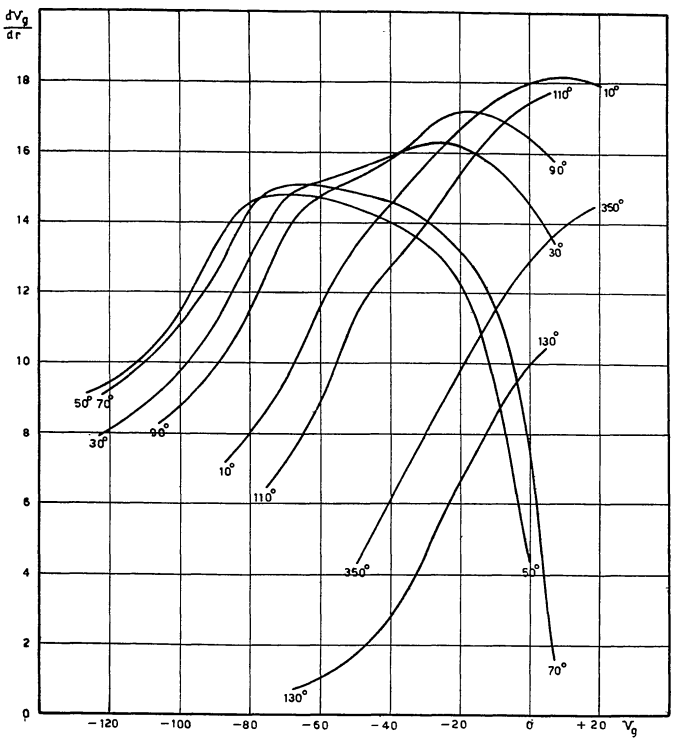

Sample curves of dV_g/dr in km/sec.kps as function of the differential rotation V_g in km/sec for various longitudes.

that used throughout the article. The thin curve gives the optical depth τ, 100 scale units being equivalent to $\tau = 1$. The broken curve gives the optical depth τ' corrected for random motions; η was assumed to be 8.5 km/sec.

18. *Density distribution in the galactic plane.*

At very large distances the layer of hydrogen will not entirely fill the antenna pattern. With an average half-width of 2°.3 a layer of effective thickness 260 ps, such as the layer of gas clouds in our vicinity, will practically fill the beam width up to a distance of 6700 ps. For the parts of the Galactic System beyond this distance corrections may have to be applied to reduce to what would have been obtained with a small beam width. It is especially in the "distant arm", observed between 345° and 50°, that we encounter distances greatly exceeding 6700 ps. However, the corrections for beam width turned out to be very much smaller than was anticipated. Sweeps across the arm at 0°, 10°, 20° and 30° longitude showed the true half-thickness of the arm to be about 3°.1, or 750 ps, therefore three times the thickness of the cloud layer in our surroundings. On the assumption that the true intensity distribution in latitude as well as the antenna pattern have a Gaussian form, the correction factor to

FIGURE 14

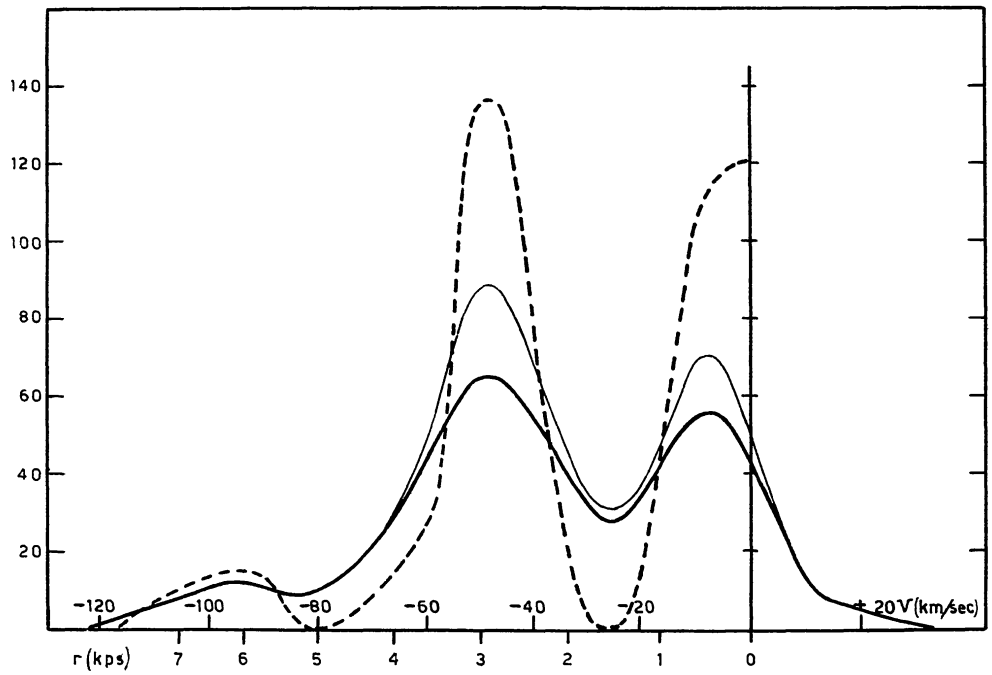

Example of reduction to optical depths and of the correction for the effect of random motions. The original profile, which is for 80° longitude, is shown by a heavy curve. The velocity scale has been indicated in km/sec, the intensity scale is in the units used throughout the present article. The thin curve shows the optical depth τ. The broken curve gives the optical depth τ' after correction for the effect of random motions. An optical depth 1 corresponds to 100 in the scale of ordinates. The scale at the bottom gives distances in kps.

zero beam width is found to be 1.17 for this arm. This factor has been applied to the intensities observed in the distant arm between 345° and 30°. The factor was, somewhat arbitrarily, assumed to decrease to 1.13 at $l = 35°$, 1.09 at 40°, 1.05 at 45°, while for $l = 50°$ and higher no corrections were applied. The thin outer arm observed between 60° and 120° longitude did not require any corrections, because also this arm appeared to be considerably thicker than the arms nearer the sun. In the region beyond 180° longitude the corrections were assumed to be negligible.

If the curves in Figure 5, or the numbers in Table 1, are transformed into optical thickness by means of (13), taking $I_0 = 110$, we can integrate $\tau(V)$ over all values of V, and thus obtain the total number of hydrogen atoms in a column of 1 cm² cross-section. Taking $T = 110°$ this total number is, according to (12),

$$N_H = \int_0^\infty n_H\, dr = 2.02 \times 10^{15} \int_0^\infty \tau(V)\, dV.$$

TABLE 5

Total number of hydrogen atoms in a column of 1 cm² cross-section, and average densities in the galactic plane.

l	N_H (10^{22} cm^{-2})	N'_H (10^{22} cm^{-2})	r (kps)	$\overline{n_H}$ (cm^{-3})
30°	2.13	1.99	12.22	.53
35	1.99	1.93	11.30	.55
40	1.99::	1.92::	10.40	
45	2.31::	2.20::	9.53	
50	1.80	1.73	8.69	.65
55	1.18	1.08	7.92	.44
60	1.39	1.19	7.21	.54
65	1.26	1.20	6.57	.59
70	0.87	0.82	6.00	.44
75	1.10	0.98	5.51	.58
80	0.97	0.88	5.06	.57
85	0.86	0.77	4.70	.53
90	0.87	0.76	4.37	.56
95	1.05	0.87	4.11	.69
100	1.03	0.88	3.89	.73
105	1.13	0.90	3.68	.79
110	1.49	1.30	3.52	1.20
115	1.48	1.12	3.38	1.08
120	1.39	1.14	3.26	1.13
125	1.16	0.84	3.14	.87
130	0.94			
135	1.14			
165	1.29::	1.09::	3.08	1.15::
170	0.91	0.76	3.18	.78
175	1.28	0.98	3.26	.98
180	0.94	0.70	3.39	.66
185	1.18	0.86	3.53	.79
190	0.84	0.62	3.73	.54
195	0.77	0.61	3.91	.51
200	1.22	0.96	4.14	.75
205	1.22	0.82	4.42	.60
210	0.87	0.63	4.76	.43
215	0.78	0.54	5.15	.34
220	1.26	0.96	5.61	.55

These values are shown under N_H in Table 5. The same table also gives, under N'_H, the estimated number in a similar column extending to the circle with radius 11.2 kps around the centre, i.e. to a distance 3 kps larger than the sun's distance from the centre. This includes the region of the Perseus arm and the distant arm. The numbers N'_H were obtained by integrating to the velocity equal to the effect of galactic rotation at that distance. The length of the column in kps is shown under r. The average number of hydrogen atoms per cm³ over this length is given under $\overline{n_H}$ in the last column. When the optical thickness becomes large its exact value cannot be determined with any certainty. For this reason the longitudes 140° — 160° have been left out, while the values for $l = 40°$ and 45° have been marked as uncertain. Leaving out these uncertain values the straight average n_H is found to be 0.68. Had we confined ourselves to the ring between $R = 8.2$ and $R = 11.2$, by leaving out $l = 30°$ and 35°, the result would have been 0.70. This includes arms as well as inter-arm regions. In the arms, as we shall see below, the density is considerably higher.

The optical thickness τ' in the absence of random motions is proportional to $\mathfrak{N}(V_g)$ by the same factor as τ is proportional to $N(V)$. Evidently, τ' can be computed from τ in the same manner as in (21) $\mathfrak{N}$ is calculated from N. Again taking $T = 110°$ we find from (12) and (18)

$$n_H(r) = 0.0655\ \tau'(V_g)\, dV_g/dr, \qquad (22)$$

where dV_g/dr is in km/sec.kps, while the relation between r and V_g, and the quantities dV_g/dr are given by curves like those shown for a few selected longitudes in Figures 10 and 13.

TABLE 6

Longitudes where η differs from 8.5 km/sec.

l	η	l	η
75°	7.0	180°	7.5
110	7.5	205	7.0
165	7.0	210	7.0
175	7.5	215	7.0*)

* for the region within 2 kps; for larger distances η was taken 8.5 km/sec.

The detailed calculations of τ' from I, and the determination of dV_g/dr have been carried out by Mr WOLTERBEEK MULLER, to whom we are much indebted for his able assistance.

The average random velocity η has generally been taken 8.5 km/sec, the value found in section 17. In some longitudes, however, this value gave clearly an overcorrection, leading to considerable negative densities. In these cases, which are listed in Table 6,

FIGURE 15

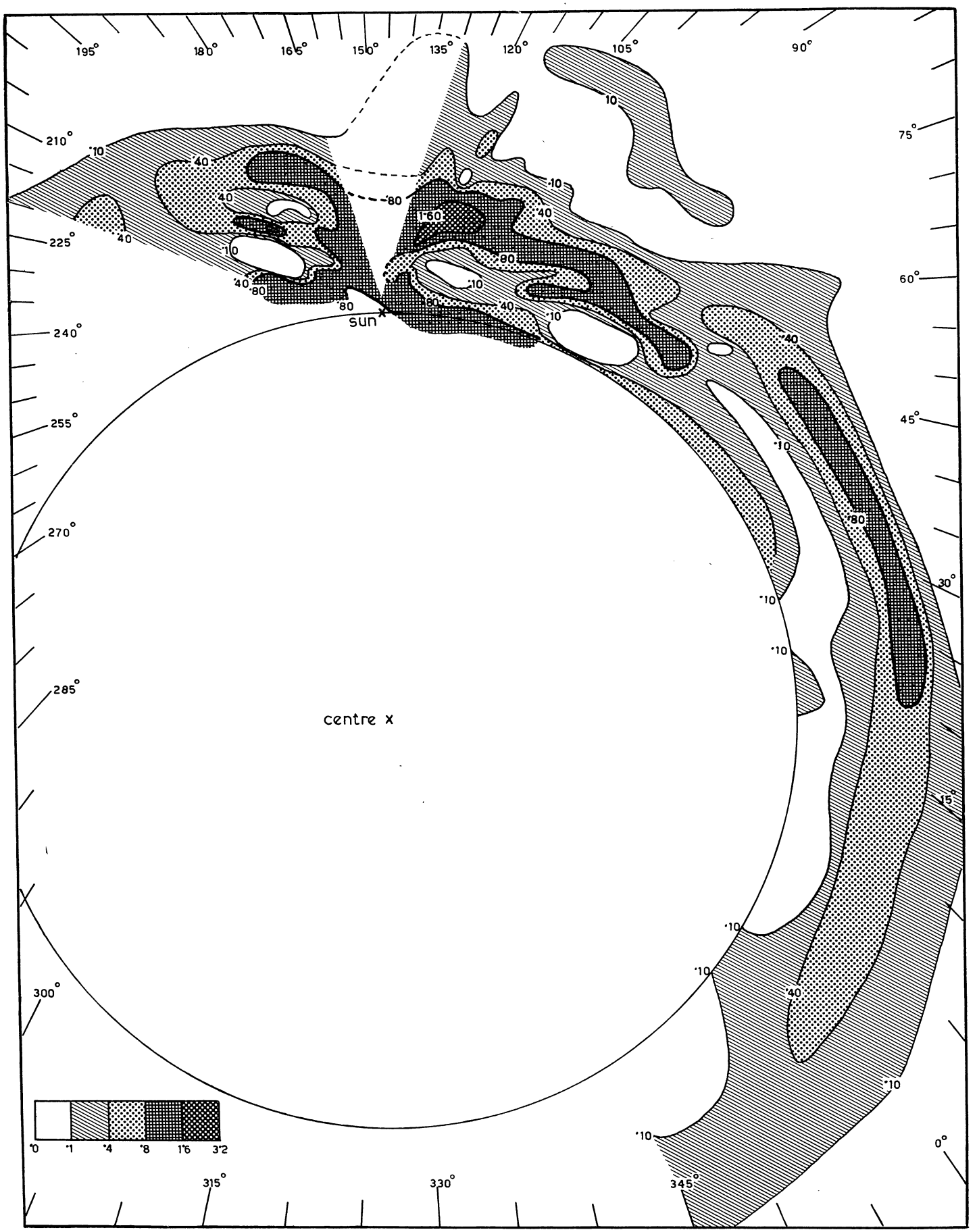

Contour map of hydrogen density in the galactic plane. Scale 1 cm = 1 kps

FIGURE 16

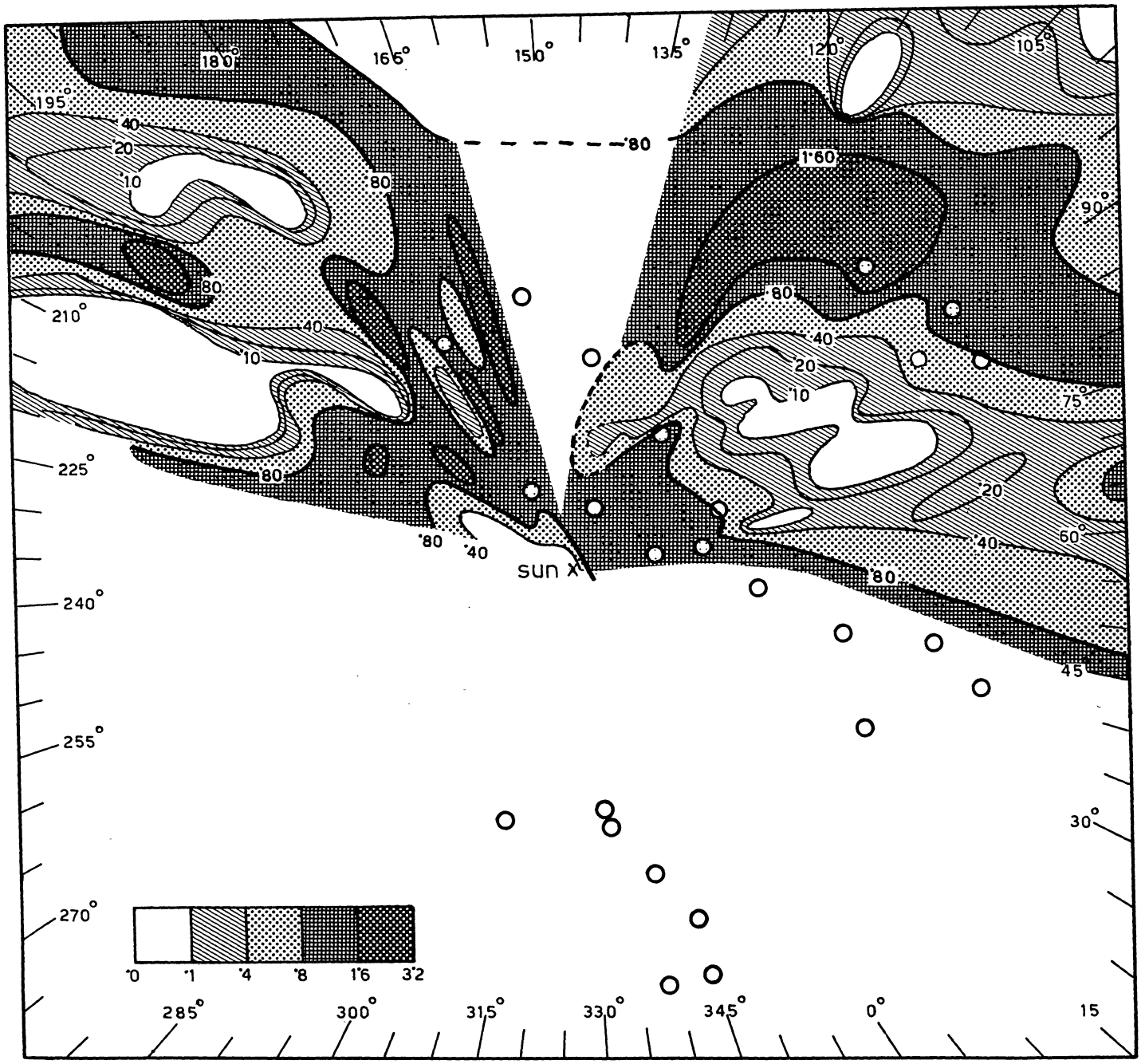

Hydrogen density in a region of 6 × 6 kps around the sun. Scale 3 cm = 1 kps. Circles indicate positions of O associations according to MORGAN, WHITFORD and CODE.

smaller values of η had to be adopted, as shown in the second and fourth columns of this table.

Maps of the hydrogen densities obtained in this way are shown in Figures 15 and 16, where points of equal density have been connected by curves. Figure 15 comprises the entire galactic plane so far as this is visible from the Netherlands. Figure 16 shows the region within 3 kps from the sun on a larger scale.

The very tentative nature of these results should be stressed. The correction for random motions is evidently a most uncertain link in the reductions. Its statistical nature makes it applicable only when there are large numbers of clouds moving independently. If we adopt BLAAUW's estimate [1]) that a line of sight of 1 kps in the galactic plane crosses 10 clouds, and if we suppose the clouds to have diameters of 10 ps, the volume surveyed in the field of our telescope, and in a velocity range corresponding to the band width of

[1]) *B.A.N.* **11**, 459, 1952.

8.4 km/sec, would contain some 20 clouds at a point in the near-by arm at 500 ps distance, and about 800 clouds at a point in the Perseus arm at 3 kps. These numbers are considerable. But it is doubtful whether the second condition, that of independent and entirely random motions is always sufficiently fulfilled. Deviations from this state are likely to appear in a much exaggerated form in the resulting values of n_H. For this reason some of the irregularities shown in Figures 15 and 16 must be expected to be fortuitous. The difficulties increase when the longitude approaches that of the centre or anticentre. The effects of differential galactic rotation then gradually decrease, and the random motions begin to wipe out all structural details. For longitudes differing less than 20° from the direction of the anticentre the arms can no longer be separated.

Accordingly, in Figures 15 and 16 the sector between 132° and 162° longitude, as well as that between 345° and the centre, has been left blank. The results for 125°, 130°, 165° and 170° are very uncertain. For instance, the long drawn-out region of high density shown in Figure 16 at $l = 165°$ may well be a combination of two separate maxima. For the sake of clarity the contours have been connected through the blank sector. These parts have been indicated by broken lines; they are largely arbitrary.

The various densities have been indicated by different shading. The average top density in the Orion arm is 1.3 for the part between 70° and 130° longitude, and 1.6 for the part between 170° and 220°. In the former longitudes the part of the arm where the density exceeds 0.8 extends from the sun to about 800 ps distance. Between 170° and 195° the density is less than 0.4 up to a distance of 180 ps, while it generally exceeds 0.80 between 350 and 2000 ps. From 200° to 220° longitude the region of low density ($n_H < 0.4$) extends to 600 ps, while the subsequent high-density region ($n_H > 0.8$) extends roughly from 800 to 1600 ps.

Between the Orion arm and the Perseus arm the density generally decreases to zero, and similarly between the Perseus arm and the "thin outer arm". The densest part of the Perseus arm occurs between 97° and 123°, where the mean top density is 2.7. The mighty association around h and χ Persei is contained in this region. Between 95° and 65° the average top intensity drops to 1.2. After this there is a break with considerably lower densities, extending to about 47°. Between the longitudes 45° and 20° the long distant arm shows top densities averaging 1.0. In the subsequent part the density seems appreciably lower: the mean top density between 355° and 15° is found to be 0.5. Nevertheless the arm is still well pronounced, being separated by a deep and wide minimum from the more inward part of the system.

Finally, the top density in the thin outer arm observed between 70° and 110° longitude is found to be about 0.12.

Between $l = 20°$ and $l = 125°$ the width of the "distant" and the Perseus arm between points where the density is half the top value is roughly 0.8 kps, this width being measured in the galactic plane in a direction perpendicular to the arm. The distance between the point where the density in the Orion arm has become half the top density and the corresponding point in the Perseus arm is about 1.2 kps in the region between 60° and 120° longitude, again measured in a direction perpendicular to the arm. Between 20° and 50° this is about 2.0 kps.

It is not unlikely that in broad features the density of hydrogen atoms will reflect that of solid particles. If this is so, the hydrogen densities may be used to estimate the absorption. We are starting an investigation on the correlation between absorption and hydrogen density. To carry this out in a satisfactory way a survey up to 10° or 20° latitude is required. This is now in progress.

19. *Comparison with other data on spiral structure.*

Large-scale features in the distribution of the gas have been investigated by MORGAN, SHARPLESS and OSTERBROCK[1]), and by GUIDO MÜNCH[2]). The former studied the distribution of regions of ionized hydrogen, and thereby found the first definite evidence for spiral structure in the Galactic System. The arrangement which they discovered follows closely the pattern of the neutral hydrogen outlined in the present article. MÜNCH's investigation refers probably to the neutral clouds. He studied the interstellar absorption lines of Na and Ca^+ in distant stars with the aid of 200-inch coudé spectrographs. He observed that stars with longitude in the range 65° to 130° and at distances of the order of 2 kps, consistently show two strong components, which he ascribed to clouds in the two principal arms. Between 85° and 115° longitude, where the differential rotation is a maximum, the average velocities of the two components are about −7 and −46 km/sec, after the solar motion has been eliminated. The former corresponds to a mean distance of 400 ps, agreeing well enough with the mean distance of the hydrogen in the Orion arm, as shown in Figure 16. The latter velocity is very nearly identical with the mean velocity of the Perseus arm as shown by the line profiles of Figure 5. This would indicate that the clouds observed by MÜNCH are distributed over the whole width of the Perseus arm.

The early-type stars have been studied extensively by W. W. MORGAN and several collaborators. A pre-

[1]) *A.J.* **57**, 3, 1952; a plot has been given in *Sky and Telescope* **11**, 134, 1952.
[2]) *Publ. A.S.P.* **65**, 179, 1953.

liminary determination of the space distribution, in particular of the O associations, has been published by MORGAN, WHITFORD and CODE [1]). The distances were based on calibrations of MORGAN's luminosity classes that are fairly independent of the distances based on differential rotation used in the present article. The associations listed by MORGAN, WHITFORD and CODE have been plotted as small circles in Figure 16, except No. 16 at $l = 71°$, $r = 3.6$ kps, that fell outside the limits of this figure. Apparently the general distribution of the associations follows the same pattern as the hydrogen. In all directions where the hydrogen density is known, the associations are observed inside or on the edge of the regions where n_H exceeds 0.8; the only exception is No. 19 in MORGAN, WHITFORD and CODE's list, which falls about 200 ps outside the .80 contour. The four associations between 40° and 50° longitude are very probably in a long stretch of dense hydrogen, as is indicated by the high 21-cm intensities observed in this direction.

The five associations in the Perseus arm are all near the inner edge of the arm as outlined by the 21-cm measures. It is possible that this is due to an effect of absorption, which blots out the far side of this arm. For the inner arm indicated by MORGAN, WHITFORD and CODE (the Sagittarius arm) no comparison with hydrogen densities is possible at present.

A direct comparison of our hydrogen densities with the distribution of O and B stars in general will have to await the publication of individual distances based on MORGAN's luminosity classes. Meanwhile we may refer to an investigation by WEAVER, based principally on radial velocities [2]). WEAVER gives, first, a comparison of our preliminary results with the distribution of open clusters, HII regions and O associations (cf. Figure 1 of his article). He uses 42 open clusters classified by TRUMPLER as IB2 or earlier. The distances rest partly on photometric data, partly on radial velocities (galactic rotation) and partly on diameters. On the whole, the distributional features of the clusters are seen to agree satisfactorily with those of the hydrogen. The distribution of early B stars, as shown in WEAVER's Figure 13, is based on observations of the distribution in longitude, and on distances derived from radial velocities. In general there is again good agreement with the hydrogen results, except for a region between 70° and 100° longitude, where WEAVER locates a structure of B stars just in between the main hydrogen arms, in a region where the overall density of hydrogen is quite low. The evidence for the existence of this extensive intermediate structure does not seem quite convincing to us. A closer study of the luminosities of the B stars would be of interest. It may be noted that the association around NGC 7380, which WEAVER, assuming the distance of the cluster to be 1.9 kps, assigns to this intermediate concentration, occurs in MORGAN, CODE and WHITFORD's list with a distance of 3.6 kps, which would locate it in the Perseus arm.

An interesting fact to which WEAVER draws attention is the scarcity of early B stars in the longitude range 110° to 145°, which possibly indicates some kind of a break in the spiral arms.

[1]) *Ap. J.* **118**, 318, 1953.

[2]) *A. J.* **58**, 177, 1953.